The LINNEAN SOCIETY of London BOTANICAL Journal of the Linnean Society

Botanical Journal of the Linnean Society, 2015, **178**, 441–466. With 8 figures

Evolutionary significance of seed structure in Alpinioideae (Zingiberaceae)

JOHN C. BENEDICT[1]*, SELENA Y. SMITH[1,2], MARGARET E. COLLINSON[3], JANA LEONG-ŠKORNIČKOVÁ[4], CHELSEA D. SPECHT[5], JULIE L. FIFE[6], FEDERICA MARONE[6], XIANGHUI XIAO[7] and DILWORTH Y. PARKINSON[8]

[1]*Department of Earth & Environmental Sciences, University of Michigan, Ann Arbor, MI 48109-1005, USA*
[2]*Museum of Paleontology, University of Michigan, Ann Arbor, MI 48109-1079, USA*
[3]*Department of Earth Sciences, Royal Holloway, University of London, London TW20 0EX, UK*
[4]*Herbarium, Singapore Botanic Gardens, National Parks Board, Singapore 259569*
[5]*Department of Plant and Microbial Biology & University and Jepson Herbaria, University of California, Berkeley, CA 94720-2465, USA*
[6]*Swiss Light Source, Paul Scherrer Institut, Villigen 5232, Switzerland*
[7]*Advanced Photon Source, Argonne National Laboratories, Argonne, IL 60439, USA*
[8]*Advanced Light Source, Lawrence Berkeley National Laboratories, Berkeley, CA 94720, USA*

Received 12 March 2014; revised 7 October 2014; accepted for publication 4 January 2015

Alpinioideae is the largest of the four subfamilies of Zingiberaceae and is widely distributed throughout the New and Old World tropics. Recent molecular studies have shown that, although Alpinioideae is a strongly supported monophyletic subfamily with two distinct tribes (Alpinieae and Riedelieae), large genera, such as *Alpinia* and *Amomum*, are polyphyletic and are in need of revision. *Alpinia* and *Amomum* have been shown to form seven and three distinct clades, respectively, but, for many of these clades, traditional vegetative and floral synapomorphies have not been found. A broad survey of seeds in Alpinioideae using light microscopy and synchrotron-based X-ray tomographic microscopy has shown that many clades have distinctive seed structures that serve as distinctive apomorphies. Tribes Riedelieae and Alpinieae can be distinguished on the basis of operculum structure, with the exception of three taxa analysed. The most significant seed characters were found to be various modifications of the micropylar and chalazal ends, the cell shape of the endotesta and exotesta, and the location of an endotestal gap. A chalazal chamber and hilar rim are reported for the first time in Zingiberaceae. In addition to characterizing clades of extant lineages, these data offer insights into the taxonomic placement of many fossil zingiberalean seeds that are critical to understanding the origin and evolution of Alpinioideae and Zingiberales as a whole. *Botanical Journal of the Linnean Society*, 2015, **178**, 441–466.

ADDITIONAL KEYWORDS: chalaza – chalazal chamber – embryo – mesotesta – micropyle – operculum – seed – *Spirematospermum* – synchrotron-based X-ray tomographic microscopy (SRXTM) – testa.

INTRODUCTION

Zingiberaceae (the gingers) is the largest of the eight families of Zingiberales, and is distributed throughout the Old and New World tropics with a centre of diversity in Asia (Larsen *et al*., 1998; Larsen, 2005). The members of the family are easily differentiated from other Zingiberales by a distinct labellum with two fused adaxial staminodes, two nectariferous glands at the base of the style and, perhaps most notably, by the presence of ethereal oils found throughout the vegetative organs of the plant, which give gingers their unique flavour and smell (Kress, 1990; Larsen *et al*., 1998; Kress *et al*., 2001; Pedersen, 2003). Traditionally, Zingiberaceae has been divided

*Corresponding author. E-mail: jcbenedi@umich.edu

into four tribes based on a suite of morphological characters; however, the characters are not uniquely distributed within a single tribe or are not present in all members of the tribe (Kress, Prince & Williams, 2002; Pedersen, 2003). To address this issue, Kress *et al*. (2002) analysed plastid *matK* and nuclear rDNA internal transcribed spacer (ITS) sequences and revised the family to include four well-supported subfamilies: two early diverging subfamilies Siphonochiloideae Kress (two genera/17 species) and Tamijioideae Kress (one genus/one species), and two large subfamilies Alpinioideae Link (20 genera/~900 species) and Zingiberoideae Haask. (30 genera/~680 species) (Harris *et al*., 2006; The Plant List, 2013).

Alpinioideae is the largest subfamily in Zingiberaceae and is characterized by having two reduced or absent lateral staminodes and a plane of distichy perpendicular to the growth of the rhizome (Burtt, 1972; Kress *et al*., 2002). The two recognized tribes in Alpinioideae, Riedelieae and Alpinieae, can be easily distinguished from each other, as members of Riedelieae possess long silique-like capsules that dehisce basally and extrafloral nectaries on the midrib of the adaxial surface of the leaf blade (Kress *et al*., 2002). In contrast, members of Alpinieae often possess globose or ovoid fruits that are not as elongated as those seen in Riedelieae and lack extrafloral nectaries (Smith, 1972, 1990b; Larsen & Mood, 1998; Kress *et al*., 2002). Although molecular and morphological data strongly support the monophyly of these two tribes, intergeneric relationships in Alpinieae are not well supported and recent studies have shown instances of paraphyly and polyphyly throughout the tribe, most notably in *Alpinia* Roxb. and *Amomum* Roxb. (Rangsiruji, Newman & Cronk, 2000a, b; Xia, Kress & Prince, 2004; Kress *et al*., 2005, 2007; Kaewrsi *et al*., 2007).

A formal revision of Alpinioideae has yet to be published to address these incongruencies in phylogenetic relationships, but well-supported informal clades based on ITS and *trnK/matK* sequence data have been proposed, and include seven distinct clades of *Alpinia* taxa [*Alpinia carolinensis* Koidz. clade, *Alpinia eubractea* K.Schum. clade, *Alpinia fax* B.L.Burtt & R.M.Sm. clade, *Alpinia galanga* (L.) Willd. clade, *Alpinia rafflesiana* Wall. clade, *Alpinia zerumbet* (Pers.) B.L.Burtt & R.M.Sm. clade and *Alpinia zerumbet* subclade] and three clades of *Amomum* (*Amomum maximum* Roxb. clade, *Amomum tsao-ko* Crevost & Lemarié clade and *Amomum villosum* Lour. clade; Kress *et al*., 2005, 2007). The proposed clades show some similarity to previous classification schemes based on morphological data (Schumann, 1904; Holttum, 1950; Wu, 1981; Smith, 1990a), but the majority are newly recognized relationships with few apomorphies, as a result, in part, of the fact that many morphological characters used to reconstruct phylogenetic trees or define lineages have been shown to be homoplasious [e.g. presence of bracteoles by Schumann (1904) and labellum shape by Smith (1990a)].

Currently, the most well-known and commonly used morphological characters for taxon identification and phylogenetic reconstruction are those from flowers and inflorescences; however, seed morphology and anatomy are also excellent sources of potentially phylogenetically informative characters (Liao & Wu, 1996, 2000; Tang *et al*., 2005), and seeds are more readily preserved as fossils than are flowers (e.g. Koch & Friedrich, 1971; Friis, 1988; Manchester & Kress, 1993; Rodriguez-de la Rosa & Cevallos-Ferriz, 1994; Fischer *et al*., 2009). Several taxonomically useful characters from fruits and seeds have been documented previously for Zingiberales (Grootjen & Bouman, 1981; Manchester & Kress, 1993; Rodriguez-de la Rosa & Cevallos-Ferriz, 1994; Liao & Wu, 1996, 2000; Liao *et al*., 2004; Tang *et al*., 2005; Benedict, 2012). In seeds, however, characters derived from the aril, operculum, micropylar collar, perisperm and endosperm, coupled with characters from seed coat anatomy, embryo shape and ovule type, have all been underutilized in understanding phylogenetic relationships and character evolution in the group (Kress *et al*., 2001, 2002, 2005, 2007). Such characters would not only be useful for the elucidation of relationships and the definition of potential synapomorphies for extant lineages, but would also facilitate the incorporation of fossil taxa into phylogenetic analyses.

The first studies of seed and fruit characters in Zingiberales can be traced back to Tschirch (1891), Humphrey (1896), Netolitzky (1926), Mauritzon (1936) and Berger (1958), whose results were summarized, together with other work, by Takhtajan (1985) to give general descriptions of the seed and fruit characters at the family level. Takhtajan (1985) noted that fruits of Zingiberaceae tend to be many seeded, are sometimes fleshy and can be loculicidally, septicidally or irregularly dehiscent. Seeds are most often anatropous, although campylotropous ovules are found in *Hedychium* J.Koenig. (Zingiberoideae) and orthotropous ovules are found in *Cucurma caulina* J.Graham (Zingiberoideae; Takhtajan, 1985). Seed coats in Zingiberaceae, and many other taxa in Zingiberales, are formed from the outer integument only (Takhtajan, 1985), and it is here that considerable anatomical variation exists. Takhtajan (1985) noted a range of 5–13 layers of cells that comprise the seed coat, but did not comment on any characters that may be useful for unifying clades in the family. Variation in seed morphology and anatomy in Zingiberaceae has not been well studied, and the only research conducted in a systematic context is that of

Liao & Wu (2000), who demonstrated differences in seed anatomy between the two large subfamilies Alpinioideae and Zingiberoideae.

The markedly revised phylogenetic hypothesis of Alpinioideae (Kress *et al*., 2005, 2007), coupled with a broad sampling of taxa within the group, allows for a reinvestigation of seed characters in a systematic context. The aim of this study is three-fold: (1) to revise and standardize the terminology previously used for Zingiberaceae seeds; (2) to assess whether there are additional variable characters that have not been utilized previously; and (3) to analyse seed characters in the context of the recently proposed phylogenetic hypothesis of Alpinioideae (Kress *et al*., 2007) to determine whether synapomorphies can be defined for the newly proposed clades.

MATERIAL AND METHODS

Forty-two species belonging to 15 genera of Alpinioideae were sampled from various herbaria, botanical gardens or purchased for use in this study (Table 1). The number of seeds available for analysis varied from one to >50 for each taxon. Specimens were either thin sectioned and observed with light microscopy, or analysed using synchrotron-based X-ray tomographic microscopy (also known as synchrotron radiation X-ray computed tomography, SRXCT). All seeds of Zingiberaceae have arils; these were not physically removed from seeds that were analysed, but, in rare cases, the aril fell off a seed during preparation for analysis.

Thin sectioning and light microscopy

Seeds of Zingiberales contain silica cells (phytoliths) that can make traditional microtomy impractical without the use of hydrofluoric acid to first dissolve the siliceous bodies (Liao & Wu, 1996, 2000). Therefore, material was embedded in Ward's Bio-plastic Synthetic Resin following the manufacturer's protocol (Ward's Natural Science, Rochester, NY, USA) and sectioned using a common protocol employed for fossilized material (Hass & Rowe, 1999; Benedict, Pigg & DeVore, 2008). Embedded seeds were longitudinally sectioned into wafers <1.0 mm thick on a Buhler Isomet low-speed lapidary saw or Buhler Isomet 1000 precision lapidary saw with a diamond blade (BUEHLER, a division of Illinois Tool Works Inc., Lake Bluff, IL, USA). Wafers were mounted on standard microscope slides using U-154 adhesive (The Company, Lakewood, CO, USA) and ground down to a minimal thickness using various grades of carborundum powder or sand paper until a single layer of cells was present on the slide. Specimens were photographed using a Nikon D70s or D90 camera body (Nikon Inc. Melville, NY, USA) attached to a Nikon SMZ 1500 stereoscope, a Nikon Eclipse E800 compound scope or a Leica DM EP compound scope with dedicated Leica DFC290 camera attachment. Images were adjusted uniformly for contrast and colour balance, and artefacts (bubbles, lint, etc.) were removed from the background only using Adobe Photoshop software version CS or CS2 (Adobe Systems Incorporated, San Jose, CA, USA).

Synchrotron-based X-ray tomographic microscopy (SRXTM)

Samples were mounted onto brass stubs or toothpicks using a PVA glue or epoxy, and imaged using standard absorption contrast at the TOMCAT beamline at the Swiss Light Source (SLS; Stampanoni *et al*., 2006; Paul Scherrer Institut, Villigen, Switzerland; specimens scanned during sessions in 2009, 2010, 2011 and 2013), the 2-BM beamline at the Advanced Photon Source (APS; Argonne National Laboratory, Lemont, IL, USA; specimens scanned during sessions in 2011 and 2012) or the 8.3.2 beamline at the Advanced Light Source (ALS; MacDowell *et al*., 2012; Lawrence Berkeley National Laboratory, Berkeley, Ca, USA; specimens scanned during session in 2013). Specimens were scanned as follows. At TOMCAT, transmitted X-rays were converted into visible light using a LAG:Ce 200-μm scintillator (2009–2011) or a 20- or 100-μm LAG:Ce scintillator (2013) screen (Crytur, Turnov, Czech Republic). Projection data were magnified by 2× or 4× microscope objectives and digitized by a high-resolution CCD camera (PCO.2000; PCO GmbH, Kelheim, Germany; 2009–2011) or sCMOS camera (PCO.edge 5.5; PCO GmbH; 2013). Samples were scanned using 10 or 13 keV and an exposure time per projection of 50, 125, 150 or 200 ms. For each scan, 1501 projections (2048 × 2048 pixels with PCO.2000 camera, 2560 × 2160 pixels with PCO.edge 5.5 camera) were acquired over 180°. Reconstruction of the tomographic data was performed on a 60-node Linux PC cluster using a highly optimized routine based on the Fourier transform method and a gridding procedure (Marone, Münch & Stampanoni, 2010; Marone & Stampanoni, 2012), resulting in a theoretical pixel size of 3.7 μm at 2× and 1.85 μm at 4× (2009–2011) or 3.25 μm at 2× and 1.625 μm at 4× (2013) for reconstructed images.

At 2-BM, transmitted X-rays were converted to visible light using a 100-μm-thick Ce-doped LAG scintillator screen (Crytur); 2.5×, 4× or 5× microscope objectives were used to magnify the projection data, and a Coolsnap K4 camera (Photometrics, Tucson, AZ, USA) was used to digitize the data. Samples were scanned at 16.1 or 21 keV with an exposure time of 280–300 ms. For each scan, 1500 projections

Table 1. List of specimens sampled and voucher information. Herbarium abbreviations follow Index Herbariorum (Thiers, continually updated)

Species	Voucher information
Aframomum daniellii (Hook.f.) K.Schum.	Delft University of Technology, JW van Loon
Aframomum melegueta K.Schum.	US, J. Higgins 44
Alpinia aquatica (Retz.) Roscoe	SING, GRC-22 and US W.J. Kress 05-7809
Alpinia boia Seem.	US, W.J. Kress 79-1071
Alpinia brevilabris C.Presl	US, M. Ramos 30411
Alpinia caerulea (R.Br.) Benth.	SING, JLS-1660
Alpinia carolinensis Koidz.	US, D.H. Lorence 7907
Alpinia conchigera Griff.	SING, GRC-205
Alpinia fax B.L.Burtt & R.M.Sm.	US, A.H.M. Jayasuriya 1217
Alpinia galanga (L.) Willd.	US, Shiu Ying Hu 6225
Alpinia haenkei C.Presl	US, A.D.E. Elmer 17662
Alpinia japonica (Thunb.) Miq.	NY, Muratailcitamura 639
Alpinia katsumadai Hayata	Delft University of Technology, JW van Loon
Alpinia luteocarpa Elmer	US, Kress & Li 05-7785
Alpinia malaccensis (Burm.f.) Roscoe	US, C. Saldanha 14771
Alpinia nigra (Gaertn.) Burtt	US, W.J. Kress 00-6808
Alpinia oblongifolia Hayata	US, J. Wen 9436
Alpinia stachyodes Hance	US, n.c., 1801
Alpinia zerumbet (Pers.) B.L.Burtt & R.M.Sm.	US, Wen 9412 and US, Fosberg 38289
Amomum aff. *glabrum*	SING, VNM-B-1479
Amomum koenigii J.F.Gmel.	SING, VNM-B-1443
Amomum lappaceum Ridl.	SING, JLS-1667
Amomum ochreum Ridl.	SING, JLS-1670
Amomum sericeum Roxb.	SING, JLS-1273
Burbidgea stenantha Ridl.	SING, GRC-88
Elettaria cardamomum (L.) Maton	Commercially purchased (JCB and SYS)
Etlingera elatior (Jack) R.M.Sm.	SING, SNG-56
Etlingera linguiformis (Roxb.) R.M.Sm.	US, W. J. Kress, M. Bordelon, T. Htum 02-7044
Etlingera yunnanensis (T.L.Wu & S.J.Chen) R.M.Sm.	SING, JLS-1717
Geostachys densiflora Ridl.	SING, JLS-1662
Hornstedtia conica Ridl.	SING, SNG-35
Hornstedtia leonurus (J.Koenig) Retz.	SING, SNG-174
Plagiostachys escritorii Elmer	NY, Elmer 16216
Plagiostachys philippinensis Ridl.	NY, Ramos & Edaño 75626
Pleuranthodium sp.	US, T.G. Hartley 10989
Renealmia lucida Maas	SING, JLS-1019
Renealmia occidentalis (Sw.) Sweet	MICH, J. Vera Santos 2513
Riedelia corallina (K.Schum.) Valeton	NY, Annable 3639
Siamanthus siliquosus K.Larsen & J.Mood	US, W.J. Kress 99-6358
Siliquamomum tonkinense Baill.	SING, VNM-B-1469
Vanoverberghia sepulchrei Merr.	NY, Ramos & Edaño 45045

(2048 × 2048 pixels) were acquired over 180°. The tomographic reconstructions were conducted with a 64-node cluster at APS using a gridrec reconstruction algorithm (Dowd *et al*., 1999). Reconstructed images had a theoretical pixel size of 2.1 μm at 2.5×, 1.7 μm at 4× and 1.5 μm at 5×.

At the 8.3.2 beamline, transmitted X-rays were converted to visible light using a 0.5-mm LuAG scintillator (Crytur). Samples were magnified with either a 2× or 5× microscope objective and digitized using a sCMOS camera (PCO.edge; PCO GmbH). Samples were scanned at 15 keV and an exposure time of 90, 500 or 950 ms. For each scan, 2049 projections (2560 × 2160 pixels) were acquired over 180°. Reconstruction was carried out using a custom ImageJ (Rasband, 1997–2014) plugin for image preprocessing and Octopus (Inside Matters, Aalst, Belgium) for tomographic reconstruction. Reconstructed images had a theoretical pixel size of 3.25 μm at 2× and 1.3 μm at 5×.

Reconstructed images were processed at the University of Michigan using Avizo 7.0 or 8.0 (FEI Visualization Science Group, Burlington, MA, USA) for Windows 7. Images were captured in Avizo 7.0 or 8.0 and edited uniformly for contrast using Adobe Photoshop CS2.

RESULTS

Variation in seed structure

Twenty-three characters were examined to describe the variation in seed structure in Alpinioideae. All seeds examined were mature, arillate, operculate with a micropylar collar, but varied in possessing a hilar rim, micropylar and chalazal mesotestal proliferation of cells, a chalazal chamber and chalazal mucro (see below, character 14). In Alpinioideae, as in all Zingiberaceae, the seed coat is derived from the outer integument only (Grootjen & Bouman, 1981) and consists of three easily distinguishable layers: the exotesta, mesotesta and endotesta (Fig. 1). A variety of terms have been used to describe zingiberalean seeds based on histological sections and surface fractures, and these are discussed below as the examined characters are introduced.

1. Seed surface. The surfaces of seeds of Alpinioideae can be striate (Fig. 2A), striate and shiny (Fig. 2B), verrucose (surfaces with small bumps, Fig. 2C) to rugose (distinctly wrinkled surfaces, Fig. 2D).

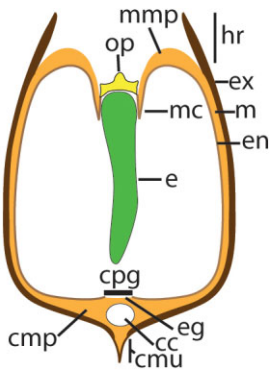

Figure 1. Stylized diagram of an Alpinioideae seed. Parts of seed colour coded as follows: embryo (green); operculum (derived from endotesta, dark yellow; derived from mesotesta, pale yellow); endotesta (light brown); mesotesta (tan); exotesta (dark brown); chalazal pigment group (black). cc, chalazal chamber; cmp, chalazal mesotestal proliferation of cells; cmu, chalazal mucro; cpg, chalazal pigment group; e, embryo; eg, endotestal gap; en, endotesta; ex, exotesta; hr, hilar rim; mc, micropylar collar; m, mesotesta; mmp, micropylar mesotestal proliferation of cells; op, operculum.

2. Seed shape. The overall shape of an individual seed in Zingiberaceae is greatly influenced by the number of seeds per locule, and taxa with multiple seeds per locule tend to have many variously shaped seeds as a result of tighter packing in the fruit (J. C. Benedict, pers. observ.). This is particularly evident in the seeds closest to the micropylar and chalazal regions, as they are often compressed during fruit and seed development. To account for this phenomenon, the following seed shapes were identified; ellipsoid (Fig. 2E–J), ovoid (Fig. 2K, L) or oblate and flattened at the poles of the seed (Fig. 2M–P).
3. Seed length. As with seed shape, seed length may also vary considerably between seeds within a single fruit, but a binary character of either 'twice as long as wide' (e.g. Fig. 2E, F, Q, R) or 'less than twice as long as wide' (e.g. Fig. 2G–P) was used to generalize seed length.
4. Seed body taper. Generally, seeds were found to taper at the chalazal region or base (Fig. 2Q, R), at the micropylar region or apex (Fig. 2K, L), at both regions or to display no tapering at all.
5. External raphe groove. Members of Zingiberales have anatropous ovules, and development of the embryo, endosperm and perisperm produces distinct external characteristics (Grootjen & Bouman, 1981). In *Costus* L., it was shown that a substantial increase in nucellus tissue enveloped the seed coat in the chalazal region, which resulted in a sunken chalaza of the mature seed (Grootjen & Bouman, 1981). It is presumed that a similar developmental event has taken place with the raphe in the mesotesta of seeds of Alpinioideae, because the seed coat is often depressed (grooved) where the raphe is located. This is apparent along a single side of the seed in many taxa (Fig. 2H, J, L, R at arrow) and, in a few taxa, this groove extends to both sides of the seed because of the presence of a post-chalazal branch of the raphe bundle (Fig. 2E, F at arrow).
6. External chalazal indentation. In some taxa, the outer surface of the chalazal region has a small circular indentation that may (Fig. 2J, L) or may not (Fig. 2H) be accompanied by the external raphe groove (character 5 above). It is unclear whether this chalazal indentation is homologous to the sunken chalaza of *Costus* (Grootjen & Bouman, 1981), and future work on the development of this trait is needed.
7. Operculum layering. An operculum is found in all taxa in Alpinioideae and is located within the tubular micropylar collar. It is a more or less conical structure formed from the inner layer(s) of the outer integument that seals the embryo cavity, and is pushed off by the embryo during

Figure 2. A–R, External morphology of seeds of Alpinioideae. A, Striate seed coat in *Alpinia boia*. B, Striate, shiny seed coat of *Aframomum melegueta*. C, Verrucose seed coat in *Alpinia luteocarpa*. D, Rugose seed coat in *Elettaria cardamomum*. E, F, *Alpinia malaccensis* seed with arrow indicating distinct 'double' raphe groove (on both sides of seed) and verrucose surface. G, H, *Elettaria cardamomum* seeds with arrow indicating distinct external raphe grove on one side of the seed. I, J, *Alpinia brevilabris* seed with arrow indicating external raphe groove and asterisk indicating chalazal indentation. K, L, *Etlingera elatior* seed with arrow indicating external raphe groove and asterisk indicating chalazal indentation. M, N, *Pleuranthodium* sp. oblate-shaped seeds and striate seed coat surface. O, *Alpinia stachyodes* seed as seen from above. P, Three-dimensional volume rendering of synchrotron-based X-ray tomographic microscopy (SRXTM) data of *A. stachyodes* showing flattening of the poles of the seed. Q, R, Elongate *Siliquamomum tonkinense* seed with prominent aril, basally tapering seed, chalazal mucro and arrow indicating external chalazal grove. Scale bars: A–D, M, N, P, 1 mm; E–L, O, 2 mm; Q, R, 5 mm. a, aril; o, operculum.

germination (Figs 3A–H, 4A–J). In all taxa observed, the sclerotic endotesta contributes to the operculum and, in some taxa, a layer of mesotestal cells also forms part of the operculum. In SRXTM images, the endotesta is often delimited by X-ray bright cells (appearing white; e.g. Figs 3B, D at arrow, 4H–J) and the mesotesta is found above this layer as either large thin-walled parenchymatous cells (Fig. 3D, H) or a dense mass of cells (Fig. 3B).

8. Micropylar collar. The micropylar collar is a cylindrical expansion of the mesotesta and endotesta into the embryonic chamber. It completely surrounds the operculum and often houses a portion of the embryo closest to the micropyle (Figs 3A–H, 4A–J). It is present in all Alpinioideae included in the current study.
9. Micropylar collar layering. As with the operculum, the micropylar collar is formed from either the endotestal cells only or both the endotestal and mesotestal cells. Three types of micropylar collar have been documented previously in Zingiberaceae based on the relative abundance of mesotestal cells in the collar (fig. 2A–C in Liao & Wu, 1996). They range from those with large-volume mesotestal cells ('form A') to those with mesotestal cells of small volume ('form B') to those with little or no mesotestal cells ('form C'). Only two micropylar collar forms were recognized in Alpinioideae: those that contain the mesotesta (Figs 3A, B, G, H, 4A–G) and those with no mesotesta (Fig. 3C–F). The distinction of large and small mesotestal cells (forms A and B) was found to be subtle and could not be determined with confidence in this study.
10. Hilar rim. The hilar rim was first described in *Ensete* Horan. (Musaceae) as a rimmed hilar depression that, in longitudinal section, 'produces the appearance of a pair of horns arising from the hilar end of the seed' (Manchester & Kress, 1993: 1267). The definition of this character has been adopted with a slight modification to define it as a tubular outgrowth of exotestal cells at the micropylar region of the seed (Fig. 4A–D, F).
11. Micropylar mesotestal proliferation. Another distinct feature of the micropylar region in some Alpinioideae is the proliferation of mesotestal cells in the micropylar region to produce a mass of cells in the shape of a three-dimensional torus or doughnut. In longitudinal section, this proliferation of cells can be seen situated between the hilar rim and micropylar collar (Fig. 4A, B, D).
12. Chalazal modification. Alpinioideae seeds range from having no cellular modifications in the chalazal region to various modifications that limit the amount of space available for the embryo and the embryo cavity (Fig. 5A–G). Chalazal modifications are divided into two general forms: chalazal chambers and testal proliferations. Chalazal chambers are empty cavities nested within the mesotesta of seed coats (Fig. 5C–F, at arrow; see character 13). Testal proliferations are masses of mesotestal cells that can fill up to almost half the volume of a mature seed (Fig. 5A–F). Testal proliferations do not include raphe and chalazal pigment group (CPG) cells (see character 21). Two types of testal proliferation exist. One is a simple mass of mesotestal cells (Fig. 5A–D, F). The other, termed here a columnar mesotestal proliferation, is a wall or column of endotestal and mesotestal cells that splits the lower portion of the embryo cavity into two segments (Fig. 5E). These two chalazal modifications are not exclusive and taxa can have both a chamber and a proliferation of mesotestal cells (Fig. 5C–F).
13. Chalazal chamber size. We observed two types of chalazal chamber in seeds of Alpinioideae: an *Alpinia*-type chamber that is less than one-third of the width of the seed (Fig. 3E), and an *Amomum*-type chamber that is defined as being one-third of the width of the seed or larger (Fig. 5C, D, F). The *Alpinia*-type chamber is restricted to the chalazal end of the seed, similar to the chalazal chambers found in Musaceae and Costaceae. In contrast, the *Amomum*-type chamber connects to a raphe canal in the mesotesta that extends to the micropylar region of the seed (Fig. 5D). This has not been reported previously, and without developmental studies it is not clear whether or not these are homologous structures. We have chosen to be conservative here and to treat them as two variations of the chalazal chamber, rather than introduce a new term without evidence for their homology.
14. Chalazal mucro. The first and only report of a chalazal mucro was by Ridley (1909), where it was termed a 'terminal mucro' and was suggested to be a modification of seeds of *Burbidgea* Hook.f. for wind and water dispersal. It is a chalazal outgrowth of the endotesta, mesotesta and exotesta that produces a distinct mucro in some seeds (Figs 2Q, R, 5H, I).
15. Palisade exotesta. The exotesta is the outermost single layer of cells of the seed coat (Fig. 6A–R). In longitudinal section, the exotesta ranges from large rectangular palisade cells to square-shaped cells (Fig. 6C–L) and to a thin layer of compressed cells that often lack cellular contents (Fig. 6M–R).
16. Uniform exotesta. The exotestal layer of cells is either a uniform layer of cells or a disorganized layer of cells that have undergone irregular

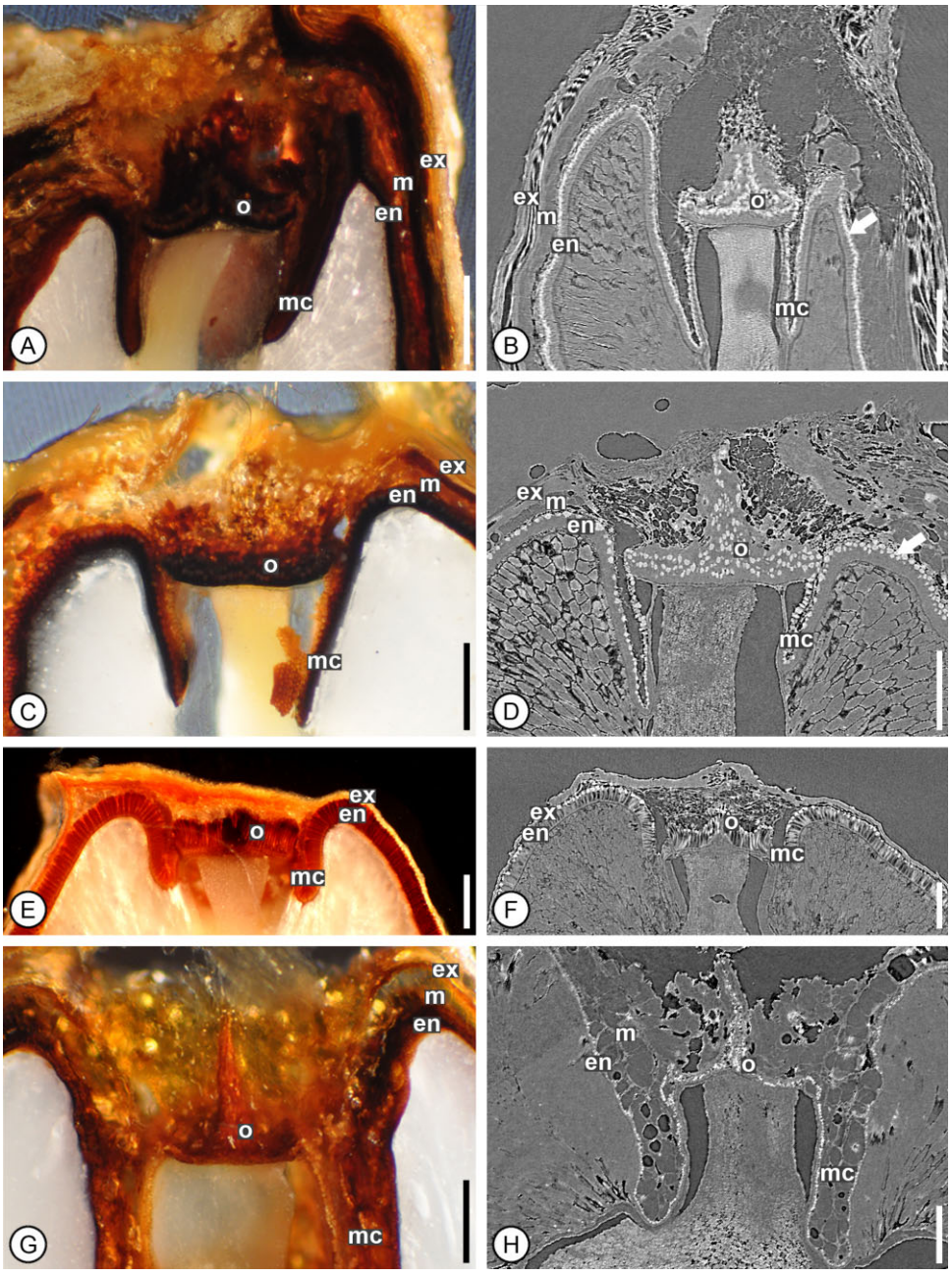

Figure 3. A–H, Variation in the operculum and micropylar collar in seeds of Alpinioideae. A, C, E, G, Light micrographs of thin sections. B, D, F, H, Digital longitudinal sections. A, B, *Alpinia boia* with palisade exotesta, bulbous mesotesta, sclerified rectangular endotestal cells, two-layered operculum and micropylar collar of endotestal cells only. Arrow, X-ray bright layer of endotestal cells. C, D, *Alpinia fax* with palisade exotesta, bulbous mesotesta, sclerified rectangular endotestal cells, two-layered operculum and micropylar collar of endotestal cells only. Arrow, X-ray bright layer of endotestal cells. E, F, *Etlingera linguiformis* with thin exotesta, thin and discontinuous mesotesta, and sclerified palisade endotesta cells that form the micropylar collar and operculum. G, H, *Alpinia nigra* with square sclerified endotesta and bulbous mesotesta that both contribute to the micropylar collar and operculum. Scale bars: 250 μm. en, endotesta; ex, exotesta; m, mesotesta; mc, micropylar collar; o, operculum.

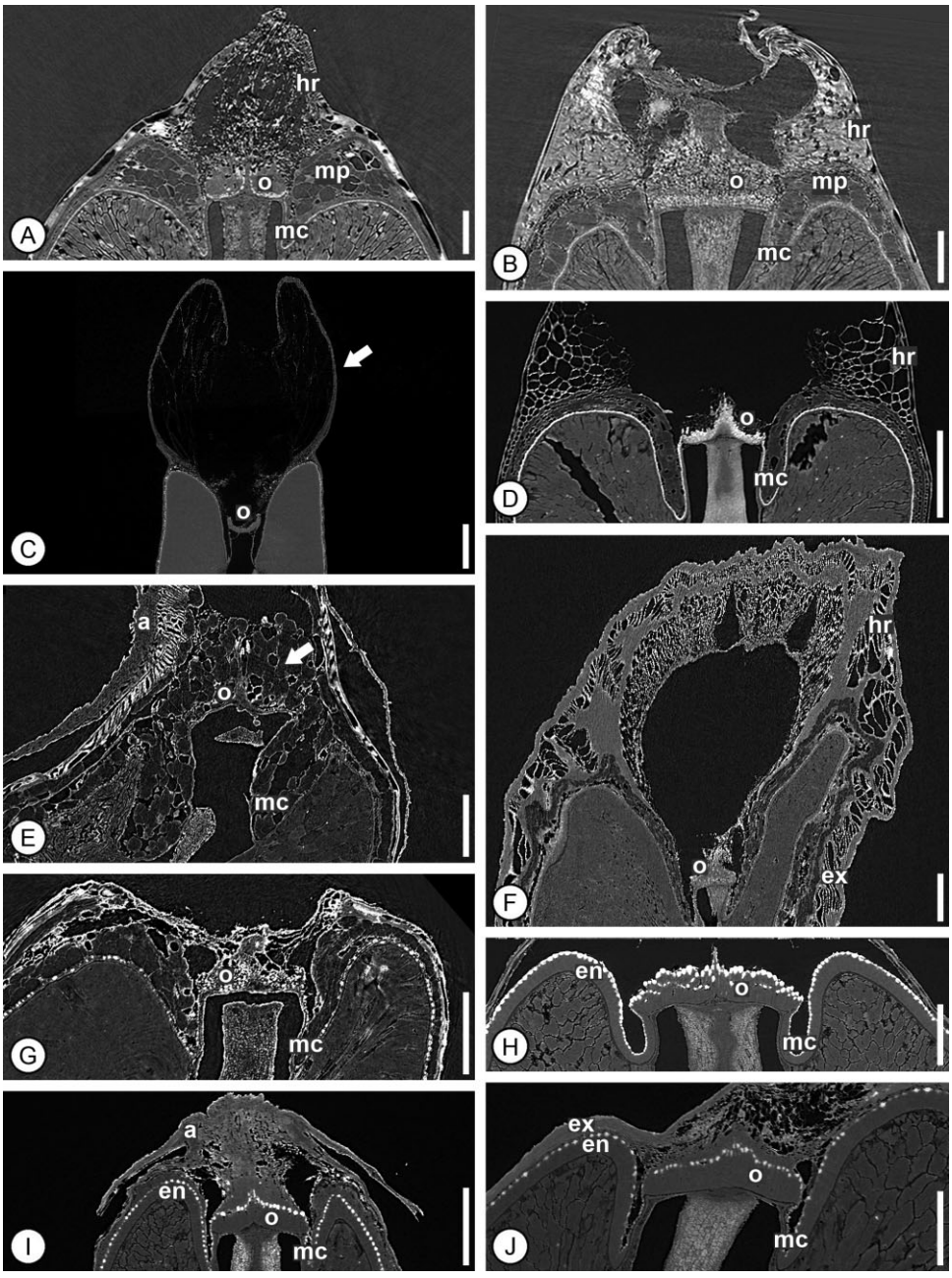

Figure 4. A–J, Digital longitudinal sections showing the variation in the micropylar region in seeds of Alpinioideae. A, *Aframomum melegueta* with hilar rim, micropylar mesotestal proliferation of cells, and micropylar collar and operculum formed of endotesta and mesotesta. B, *Aframomum daniellii* with hilar rim, micropylar mesotestal proliferation of cells, and micropylar collar and operculum formed of endotesta and mesotesta. C, *Siliquamomum tonkinense*; note hilar rim at arrow. D, *Renealmia lucida* with hilar rim, and micropylar collar and operculum formed from mesotesta and endotesta. E, *Riedelia coralline*; note bulbous second layer of tissue of the operculum (arrow) derived from the mesotesta. F, *Amomum ochreum* with large hilar rim formed from exotesta. G, *Vanoverberghia sepulchrei* with operculum and micropylar collar formed from endotesta and mesotesta. H, *Amomum sericeum* with operculum and micropylar collar made up of palisade endotesta only. I, *Hornstedtia conica* with operculum formed from two layers and micropylar collar made up of palisade endotesta only. J, *Hornstedtia leonurus* with operculum and micropylar collar formed from palisade endotesta and mesotesta. Scale bars: A–D, 250 μm; E, 150 μm; F, 500 μm; G–J, 100 μm. a, aril; en, endotesta; ex, exotesta; hr, hilar rim; mc, micropylar collar; mp, micropylar mesotestal proliferation of cells; o, operculum.

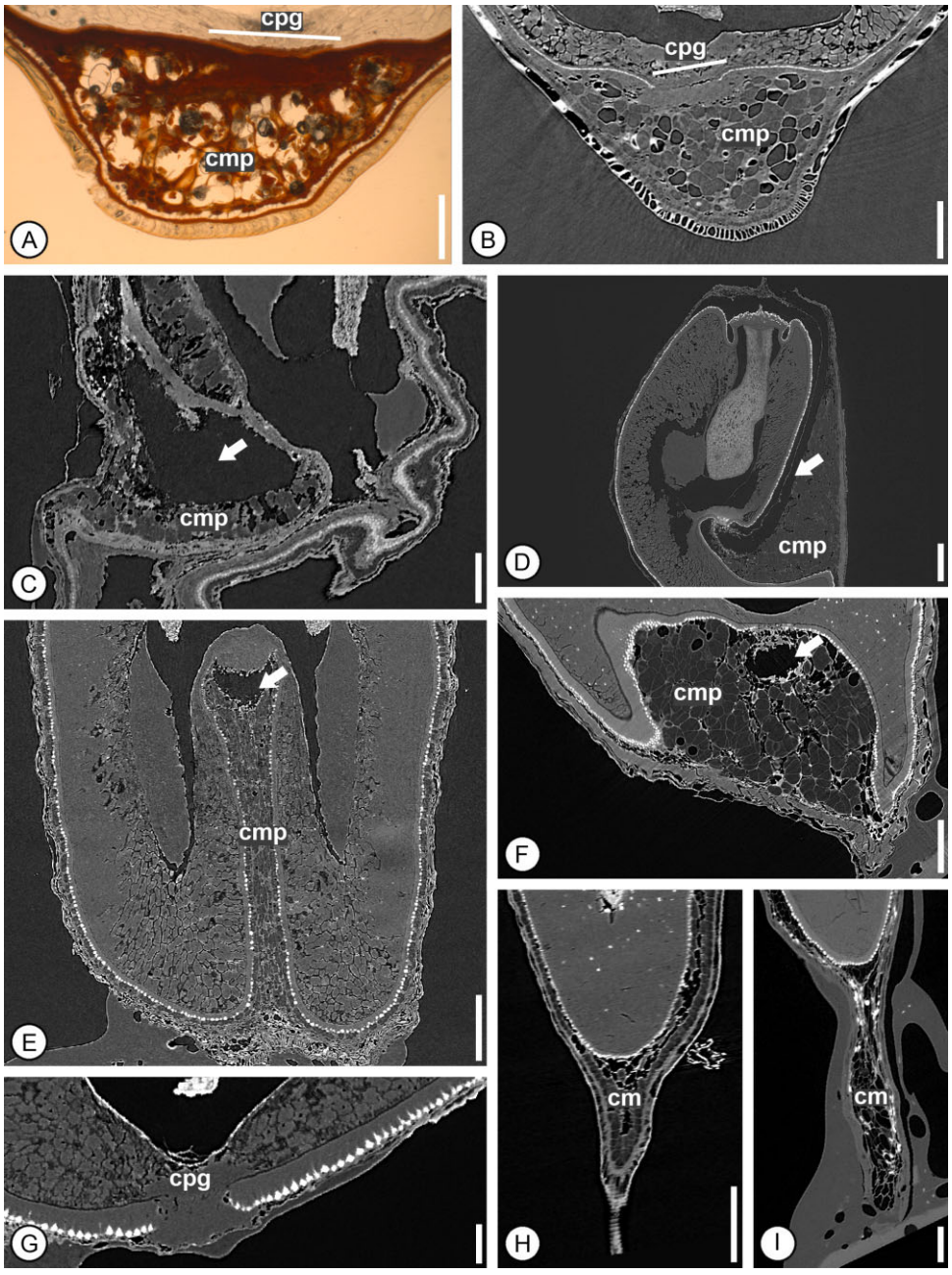

Figure 5. A–I, Variation in the chalazal region in seeds of Alpinioideae. A, Light micrograph of thin section. B–I, Digital longitudinal sections. A, B, *Aframomum melegueta* with chalazal pigment group and raphe in the endotestal gap and chalazal mesotestal proliferation of cells at the base of the seed. C, *Plagiostachys escritorii* with chalazal mesotestal proliferation of cells and *Amomum*-type chalazal chamber (arrow). D, *Amomum sericeum* with chalazal mesotestal proliferation of cells and *Amomum*-type chalazal chamber (arrow). E, *Alpinia malaccensis* with a columnar mesotestal proliferation of cells in the chalaza and *Alpinia*-type chalazal chamber (arrow). F, *Geostachys densiflora* with chalazal mesotestal proliferation of cells and *Amomum*-type chalazal chamber (arrow). G, *Etlingera elatior* with palisade endotesta and chalazal pigment group of cells between endotestal gap. H, *Burbidgea stenantha* with a chalazal mucro. I, *Siliquamomum tonkinense* with a chalazal mucro (surrounded by glue, darker grey and non-cellular). Scale bars: A–C, E, F, H–I, 250 μm; G, 100 μm; D, 500 μm. cpg, chalazal pigment group; cm, chalazal mucro; cmp, chalazal mesotestal proliferation of cells.

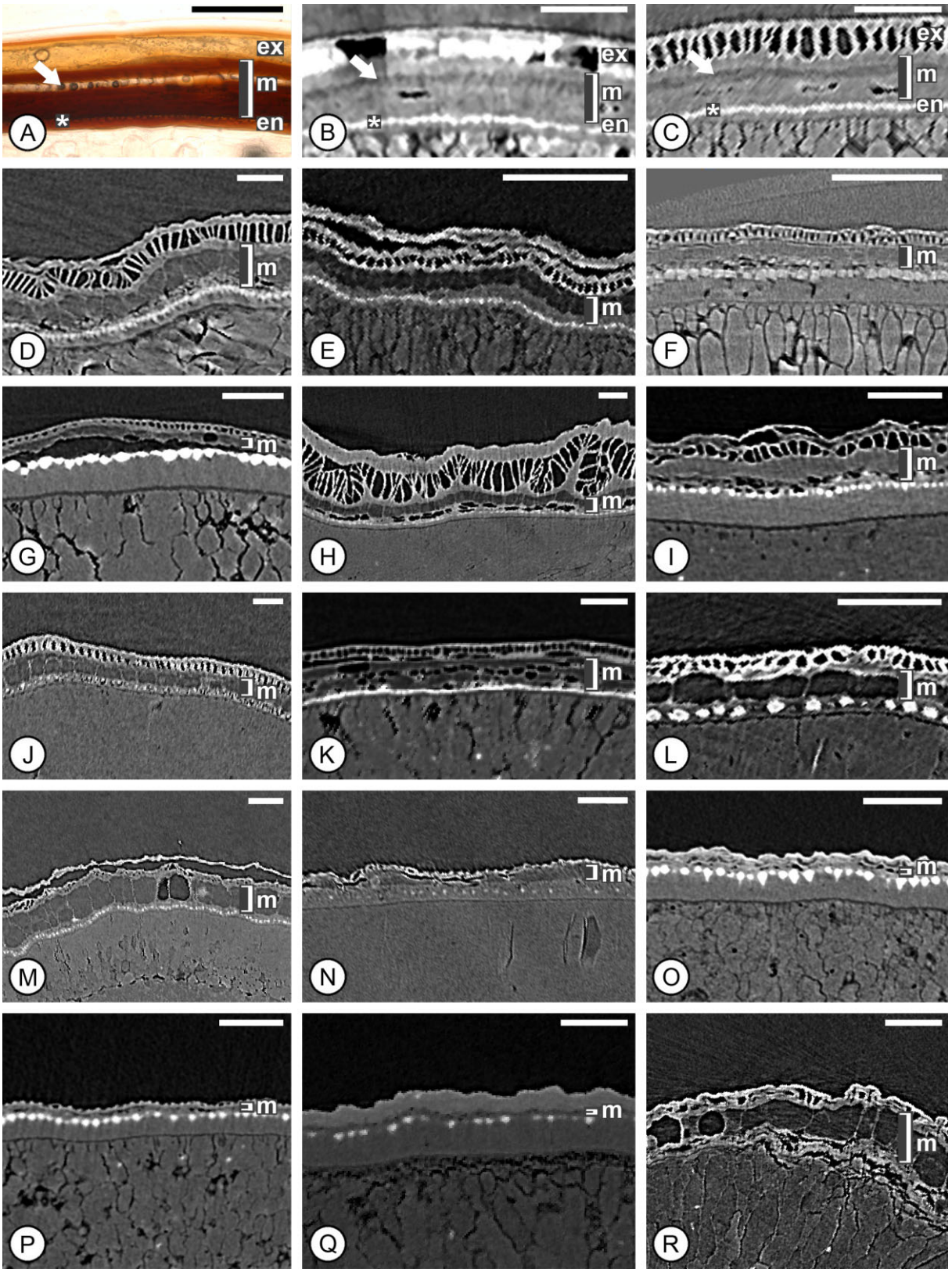

Figure 6. See caption on next page.

Figure 6. A–R, Seed coat variation in Alpinioideae. A, Light micrograph of thin section. B–R, Digital longitudinal sections. A–C, *Aframomum melegueta* seed in transverse section (A, B) and longitudinal section (C) with palisade exotesta (ex), three-layered mesotesta (m) consisting of pigmented hypodermis below exotesta, translucent layer of cells below hypodermis (arrow), and pigmented layer below translucent layer, and endotesta (en) of square sclereids capped by a small transparent layer that is X-ray bright (*). D, *Alpinia boia* with a palisade exotesta, mesotesta of large bulbous cells and endotesta of rectangular sclereids. E, *Alpinia caerulea* with a palisade exotesta, mesotesta of large bulbous cells and endotesta of square sclereids. F, *Alpinia galanga* with a palisade exotesta, mesotesta of large bulbous cells and endotesta of rectangular sclereids. G, *Amomum sericeum* with a palisade exotesta, thin mesotesta of bulbous cells and endotesta of rectangular sclereids. H, *Amomum ochreum* with a palisade exotesta, thin mesotesta of bulbous cells and endotesta of square sclereids. I, *Geostachys densiflora* with a palisade exotesta, mesotesta of bulbous cells and endotesta of rectangular sclereids. J, *Pleuranthodium* sp. with a palisade exotesta, thin mesotesta of bulbous cells and endotesta of square sclereids K, *Renealmia lucida* with a palisade exotesta, mesotesta of bulbous cells and endotesta of square sclereids. L, *Vanoverberghia sepulchrei* with a palisade exotesta, mesotesta of bulbous cells and endotesta of square sclereids. M, *Alpinia nigra* with non-uniform exotesta of palisade cells, bulbous mesotesta and endotesta of square cells. N, *Alpinia brevilabris* with non-uniform exotesta of palisade cells, bulbous mesotesta and endotesta of square cells. O, *Etlingera elatior* with non-uniform exotesta, reduced mesotesta and endotesta of palisade cells. P, *Hornstedtia conica* with palisade exotesta, mesotesta of bulbous cells and endotesta of palisade sclereids. Q, *Hornstedtia leonurus* with reduced, non-uniform exotesta and mesotesta, and mesotesta of palisade cells. R, *Riedelia corallina* with non-uniform exotesta of palisade cells, large bulbous mesotesta and endotesta of square sclereids. Scale bars, 100 μm. m, mesotesta.

anticlinal divisions (e.g. Fig. 6H). The uniformity of the exotesta may also be interrupted by an inconsistent expansion of the exotesta cells, which results in a wavy appearance of the exotesta in transverse section (Fig. 6I).

17. Large mesotestal cells. The mesotesta often comprises three distinct layers of cells, which have been described as the hypodermis, the translucent cell layer and the pigment cell layer (Liao & Wu, 1996, 2000). The hypodermis is a single layer of cells adjacent to the exotesta and consists of cells with brown pigments (Fig. 6A). The translucent layer is also a single layer of cells, but without any pigments (Fig. 6A at arrow). The pigment layer can range from two to five or more cells thick and is adjacent to the endotesta. It is sometimes absent or reduced to small cells (Fig. 6G, O, Q) or consists of large cells that account for a large portion of the seed coat (Fig. 6A–F, J–M, R).
18. Endotestal cell shape. The endotesta is the innermost layer of the seed coat and is typically a single layer of sclerified cells often with lumen contents in the outermost zone that are X-ray bright in SRXTM images. These cells range in shape from square (Fig. 6A–C) to rectangular (Fig. 6D, F) and, in some taxa, they are elongated into a layer of endotestal palisade cells (Fig. 3O–Q).
19. Uniform endotesta. The endotesta is often a uniform layer of cells throughout the seed coat, but sometimes this layer has regions that are differentially elongated, causing an irregular endotestal layer. This layer has been shown to be irregular in the literature (Chen *et al.*, 1989; fig. 1.5 of Liao & Wu, 1994), but no taxa analysed here have regions of endotesta that are differentially elongated.
20. Endotestal gap location. In the chalazal region of a seed, the endotesta often contains a small circular or ellipsoid hole devoid of sclerenchymatous cells that represents the point at which the raphe terminates in the seed (Liao & Wu, 2000; Fig. 5A–G). The endotestal gap is either located at the centre of the chalazal region (Fig. 5A–C, E, G) or is situated on the side of the seed (Fig. 5D, F).
21. Chalazal pigment group (CPG) and raphe. The CPG (Liao & Wu, 1996, 2000) is a collection of cells that is located above the endotestal gap and is adjacent to the raphe (Fig. 5A–G). The shape of the CPG has been shown to vary in Zingiberaceae, and is discoid in Alpinioideae and 'trumpet shaped' in Zingiberoideae (Liao & Wu, 2000). In SRXTM images, the raphe and CPG are difficult to differentiate and are scored together.
22. Embryo shape. Four basic embryo shapes were observed in alpinioid seeds: straight and elongate (Fig. 7A); L-shaped (Fig. 7B–D); basally bulbous (Fig. 7E); and forked, with the base of the embryo splitting into two halves (Fig. 7F).
23. Embryo–endotesta contact. The embryo, perisperm and endosperm fill the embryo cavities of seeds of Alpinioideae, and the embryo can be in direct contact with the seed coat (Fig. 7G) or completely surrounded by endosperm and perisperm and not touching the endotesta (Fig. 7H). In some samples, the embryo does not fill the embryo cavity and an airspace is present between the embryo and seed coat (Fig. 7I). Embryos of

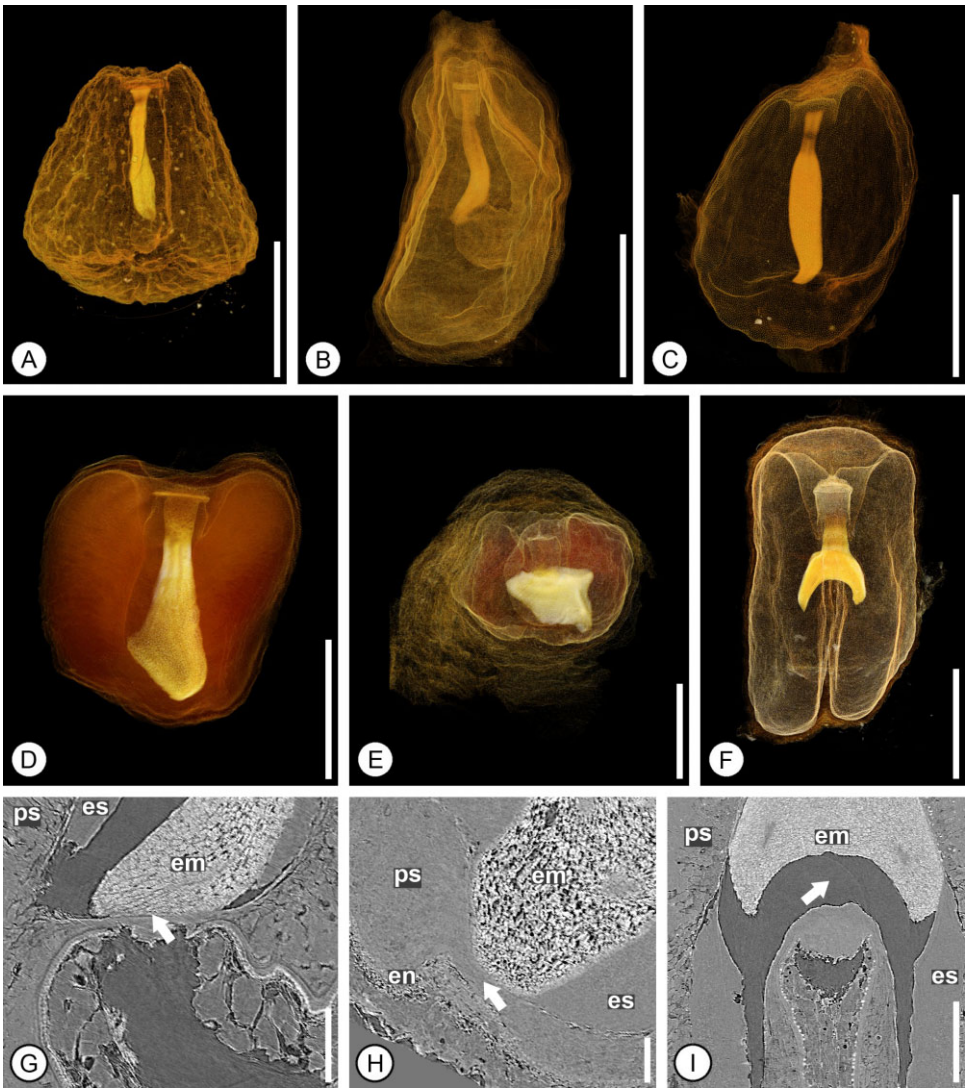

Figure 7. A–I, Embryo shape and contact with endotesta. A–F, Volume rendering of three-dimensional synchrotron-based X-ray tomographic microscopy (SRXTM) data. G–I, Digital longitudinal sections. A, *Etlingera yunnanensis* with straight embryo. B, *Alpinia boia* with L-shaped embryo. C, *Hornstedtia leonurus* with L-shaped embryo. D, *Alpinia luteocarpa* with L-shaped embryo. E, *Alpinia nigra* with basally bulbous embryo (view of top of embryo obstructed by micropylar collar). F, *Alpinia malaccensis* with forked embryo. G, *Alpinia boia*; note embryo in contact with endotesta (arrow). H, *Alpinia luteocarpa*; note embryo nested in nutrient tissue and not in contact with endotesta (arrow). I, *Alpinia malaccensis*; note embryo not in contact with endotesta and a cavity exists between embryo and endotesta (arrow). Scale bars: A–F, 2 mm; G–I, 150 μm. em, embryo; en, endotesta; es, endosperm; ps, perisperm.

these seeds are mature and considered as not touching the seed coat.

Seeds of Alpinioideae in their systematic context

Clades in parentheses correspond to those described in Kress *et al*. (2007). Results are summarized in Tables 2 and 3. No taxa were sampled from the *Alpinia rafflesiana* clade (clade 'a'), *Elettariopsis* Baker in Hook.f. clade (clade 'e'), *Amomum tsao-ko* clade (clade 'j') or *Geocharis* (K.Schum.) Riedl. clade (clade 'm') because of a lack of material.

Riedelieae clade – Riedelia *Oliv. (one species analysed)*

Riedelia corallina (K. Schum) Valeton seeds are ellipsoid, taper slightly at the base and apex, and have a striated surface. They are less than twice as long as they are wide and lack an external raphe groove and chalazal indentation. The micropylar collar comprises

Table 2. External character states of the seeds studied. ERG, external raphe groove; ECI, external chalazal indentation; +, present; –, absent; ?, unknown

Tribe	Kress 2007 clade	Taxon	Surface	Shape	Twice as long as wide	Tapering	ERG	ECI
Alpinieae	*Aframomum*	*Aframomum daniellii*	Shiny and striate	Ellipsoid	–	Base and apex	–	–
Alpinieae	*Aframomum*	*Aframomum melegueta*	Shiny and striate	Ellipsoid	–	Base and apex	–	–
Alpinieae	*Alpinia carolinensis*	*Alpinia boia*	Striate	Ovoid	–	Apex	–	–
Alpinieae	*Alpinia carolinensis*	*Alpinia carolinensis*	Shiny and striate	Ovoid	–	Base	–	–
Alpinieae	*Alpinia eubractea*	*Alpinia caerulea*	Verrucose	Ellipsoid	–	Base	+	+
Alpinieae	*Alpinia eubractea*	*Alpinia luteocarpa*	Verrucose	Ellipsoid	–	Base	–	–
Alpinieae	*Alpinia eubractea*	*Vanoverberghia sepulchrei*	Shiny and striate	Ovoid/ellipsoid	–	Base	–	–
Alpinieae	*Alpinia fax*	*Alpinia fax*	Shiny and striate	Ellipsoid	–	–	–	–
Alpinieae	*Alpinia galanga*	*Alpinia conchigera*	Shiny(?) and striate	Oblate	–	–	–	–
Alpinieae	*Alpinia galanga*	*Alpinia galanga*	Shiny and striate	Oblate	–	–	–	–
Alpinieae	*Alpinia galanga*	*Alpinia nigra*	Verrucose	Oblate	–	–	+	–
Alpinieae	*Alpinia zerumbet*	*Alpinia aquatica*	Striate	Oblate/ellipsoid	–	–	+	+
Alpinieae	*Alpinia zerumbet*	*Alpinia brevilabris*	Verrucose	Ellipsoid	–	–	+	+
Alpinieae	*Alpinia zerumbet*	*Alpinia japonica*	Striate	Ellipsoid	–	–	–?	–?
Alpinieae	*Alpinia zerumbet*	*Alpinia stachyodes*	Shiny and striate	Oblate	–	–	+	+
Alpinieae	*Alpinia zerumbet* subclade	*Alpinia haenkei*	Striate	Ellipsoid	–	–	Double	–
Alpinieae	*Alpinia zerumbet* subclade	*Alpinia malaccensis*	Verrucose	Ellipsoid	+	–	Double	–
Alpinieae	*Alpinia zerumbet* subclade	*Alpinia zerumbet*	Verrucose	Ovoid	–	–	Double	–
Alpinieae	*Alpinia zerumbet* subclade *Plagiostachys*	*Plagiostachys escritorii*	Striate	Ovoid	–	Base	–	–
Alpinieae	*Alpinia zerumbet* subclade *Plagiostachys*	*Plagiostachys philippinensis*	Striate	Ellipsoid	–	Base	–	–
Alpinieae	*Amomum maximum*	*Amomum aff. glabrum*	Rugose	Ellipsoid	–	–	–	–
Alpinieae	*Amomum maximum*	*Amomum sericeum*	Striate	Ovoid	–	Base and apex	+	–
Alpinieae	*Amomum villosum*	*Amomum koenigii*	Striate	Ellipsoid	–	Apex	–	–
Alpinieae	*Amomum villosum*	*Amomum lappaceum*	Verrucose	Ellipsoid	+	–	–	–
Alpinieae	*Amomum villosum**	*Amomum ochreum*	Striate	Ellipsoid	+	Apex	–	–
Alpinieae	*Elettaria*	*Elettaria cardamomum*	Rugose	Ellipsoid	–	–	+	–
Alpinieae	*Etlingera*	*Etlingera elatior*	Striate	Ellipsoid	–	Base and apex	+	+
Alpinieae	*Etlingera*	*Etlingera linguiformis*	Verrucose	Ovoid	–	Apex	+	+
Alpinieae	*Etlingera*	*Etlingera yunnanensis*	Verrucose	Ovoid	–	Apex	+	+
Alpinieae	*Geostachys*	*Geostachys densiflora*	Verrucose	Ovoid	–	Base	–	–
Alpinieae	*Hornstedtia*	*Hornstedtia conica*	Striate	Ellipsoid	–	Apex	+	+
Alpinieae	*Hornstedtia*	*Hornstedtia leonurus*	Striate	Ellipsoid	–	–	+	+
Alpinieae	*Renealmia*	*Renealmia lucida*	Striate	Ellipsoid	–	Base	–	–
Alpinieae	*Renealmia*	*Renealmia occidentalis*	Striate	Ovoid	–	Base	–	–
Alpinieae	Unknown clade	*Alpinia katsumadai*	Verrucose	Ellipsoid	+	–	Double	–?
Alpinieae	Unknown clade	*Alpinia oblongifolia*	Verrucose	Oblate	–	–	Double	–
Incertae sedis	*Siliquamomum*	*Siliquamomum tonkinense*	Striate	Ellipsoid	+	Base	+	–
Riedelieae	*Riedelia*	*Riedelia corallina*	Striate	Ellipsoid	–	Base and apex	–	–
Riedelieae	*Burbidgea*	*Burbidgea stenantha*	Striate	Ellipsoid	+	Base	–	–
Riedelieae	*Pleuranthodium*	*Pleuranthodium* sp.	Shiny and striate	Oblate	–	–	–	+
Riedelieae	*Siamanthus*	*Siamanthus siliquosus*	Verrucose	Ovoid	–	Base	–	–

Table 3. Internal structural features of Alpinioideae seeds. OL, operculum layering; MC, micropylar collar; MCO, micropylar collar origin; HR, hilar rim; MMP, micropylar mesotestal proliferation of cells; C mod type, chalazal modification type; CM, chalazal mucro; PE, palisade endotesta; U exo, uniform exotesta; meso, mesotesta; Uni endo, uniform endotesta; endo, endotesta; loc, location; CPG, chalazal pigment group of cells; prolif, proliferation; n/a, not applicable; +, present; –, absent; ?, unknown

Taxon	OL	MC	MCO	HR	MMP	C Mod	C mod type	Chamber type	CM	PE	U exo	Large meso	Endo shape	Uni endo	Endo gap	Endo gap loc	CPG and raphe	Embryo–endo contact	Embryo shape
Aframomum daniellii	2	+	Endo and meso	+	+	+	Meso prolif	n/a	–	+	+	+	Square	+	+	Base	+	–	Straight
Aframomum melegueta	2	+	Endo and meso	+	+	+	Meso prolif	n/a	–	+	+	+	Square	+	+	Base	+	–	Straight
Alpinia boia	2	+	Endo	–	–	+	Meso prolif and chamber	*Amomum*-type	–	+	–	+	Rectangle	+	+	Side	+	+	L-shaped
Alpinia carolinensis	2	+	Endo and meso	–	–	+	Meso prolif and chamber	*Alpinia*-type	–	+	+	+	Rectangle	+	+	Side	+	–	L-shaped
Alpinia caerulea	2	+	Endo and meso	–	–	–	n/a	n/a	–	+	+	+	Square	+	+	Side	+	–	L-shaped
Alpinia luteocarpa	2	+	Endo and meso	–	–	–	n/a	n/a	–	–	–	+	Square	+	+	Side	+	–	L-shaped
Vanoverberghia sepulchrei	2	+	Endo and meso	–	–	+	Meso prolif	n/a	–	+	+	+	Square	+	+	Side	+	–	Straight
Alpinia fax	2	+	Endo	–	–	+	Meso prolif and chamber	*Alpinia*-type	–	+	+	+	Rectangle	+	+	Side	+	–	Straight
Alpinia conchigera	2	+	Endo and meso	–	–	+	Meso prolif	n/a	–	+	+	+	Rectangle	+	+	Base	+	–	Basally bulbous
Alpinia galanga	1	+	Endo and meso	–	–	+	Meso prolif	n/a	–	+	+	+	Rectangle	+	+	Base	+	–	L-shaped
Alpinia nigra	2	+	Endo and meso	–	–	+	Meso prolif	n/a	–	–	–	+	Square	+	+	Base	+	–	Basally bulbous
Alpinia aquatica	2	+	Endo and meso	–	–	–	n/a	n/a	–	–	+	+	Square	+	+	Side	+	–	L-shaped
Alpinia brevilabris	2	+	Endo and meso	–	–	–	n/a	n/a	–	–	–	+	Square	+	+	Side	+	–	L-shaped
Alpinia japonica	2	+	Endo	–	–	+	Meso prolif and chamber	*Alpinia*-type	–	–	–	+	Rectangle	+	+	Side	+	–	L-shaped
Alpinia stachyodes	2	+	Endo and meso	–	–	+	Meso prolif	n/a	–	+	+	+	Rectangle	+	+	Base	+	–	L-shaped
Alpinia haenkei	2	+	Endo and meso	–	–	+	Columnar meso prolif and chamber	*Alpinia*-type	–	+	–	+	Square	+	+	Base	+	–	Forked
Alpinia malaccensis	2	+	Endo and meso	–	–	+	Columnar meso prolif and chamber	*Alpinia*-type	–	+	–	+	Rectangle	+	+	Base	+	–	Forked
Alpinia zerumbet	2	+	Endo and meso	–	–	+	Columnar meso prolif and chamber	*Amomum*-type	–	–	–	+	Square	+	+	Base	+	–	Forked (slightly)
Plagiostachys escritorii	2	+	Endo and meso	–	–	+	Meso prolif and chamber	*Amomum*-type	–	+	+	+	Square	+	+	Side	+	–	Straight
Plagiostachys philippinensis	2	+	Endo	–	–	+	Meso prolif and chamber	*Amomum*-type	–	–	+	+	Square	+	+	Side	+	–	Straight
Amomum aff. *glabrum*	1	+	Endo	–	–	–	n/a	n/a	–	+	+	–	Rectangle	+	+	Base	+	–	Straight
Amomum sericeum	1	+	Endo	–	–	+	Meso prolif and chamber	*Amomum*-type	–	+	+	+	Rectangle	+	+	Side	+	–	L-shaped
Amomum koenigii	2	+	Endo	–	–	+	Meso prolif	n/a	–	–	+	+	Rectangle	+	+	Side	+	–	Straight
Amomum lappaceum	2	+	Endo	–	–	+	Meso prolif	n/a	–	+	+	+	Rectangle	+	+	Side	+	–	Straight
Amomum ochreum	2	+	Endo and meso	+	–	+	Meso prolif and chamber	*Alpinia*-type	–	+	–	+	Square	+	+	Side	+	–	Straight
Elettaria cardamomum	2	+	Endo	–	–	+	Meso prolif	n/a	–	+	+	+	Rectangle	+	+	Side	+	–	L-shaped
Etlingera elatior	1	+	Endo	–	–	–	n/a	n/a	–	–	–	–	Palisade	+	+	Base	+	–	L-shaped
Etlingera linguiformis	2	+	Endo	–	–	–	n/a	n/a	–	–	–	–	Palisade	+	+	Base	+	–	L-shaped
Etlingera yunnanensis	1	+	Endo	–	–	–	n/a	n/a	–	–	–	–	Palisade	+	+	base	+	–	Straight
Geostachys densiflora	2	+	Endo	–	–	+	Meso prolif and chamber	*Amomum*-type	–	+	–	+	Rectangle	+	+	Side	+	–	L-shaped
Hornstedtia conica	2	+	Endo and meso	–	–	+	Meso prolif	n/a	–	+	+	+	Palisade	+	+	Base	+	–	L-shaped
Hornstedtia leonurus	2	+	Endo	–	–	–	n/a	n/a	–	–	–	–	Palisade	+	+	Base	+	–	L-shaped
Renealmia lucida	2	+	Endo and meso	+	–	+	Meso prolif and chamber	*Alpinia*-type	–	+	+	+	Square	+	+	Base	+	–	L-shaped
Renealmia occidentalis	2	+	Endo and meso	+	–	+	Meso prolif and chamber	*Amomum*-type	–	+	+	+	Square	+	+	Base	+	–	Straight
Alpinia katsumadai	2	+	Endo and meso	–	–	+	Columnar meso prolif and chamber	*Alpinia*-type	–	+	–	+	Square	+	+	Base	+	–	Forked
Alpinia oblongifolia	2	+	Endo	–	–	+	Columnar meso prolif and chamber	*Alpinia*-type	–	–	–	+	Rectangle	+	+	Base	+	–	Forked
Siliquamomum tonkinense	1	+	Endo and meso	+	–	–	n/a	n/a	+	+	+	–	Rectangle	+	+, oval	Side	+	–	Straight
Riedelia corallina	2	+	Endo and meso	–	–	–	n/a	n/a	–	+	–	+	Square	+	+	Side?	+ ?	–	Straight
Burbidgea stenantha	2	+	Endo	+	+	–	n/a	n/a	+	+	+	+	Square	+	+	Side	+	–	Straight
Pleuranthodium sp.	2	+	Endo and meso	–	–	+	Meso prolif	n/a	–	+	+	+	Square	+	+	Base	+	–	Straight
Siamanthus siliquosus	2	+	Endo	–	–	–	n/a	n/a	–	+	–	+	Rectangle	+	+	Base	+	–	L-shaped

both the endotesta and mesotesta. A hilar rim and micropylar mesotestal proliferation of cells are both absent. The operculum is formed from two layers of the testa, with the outermost layer being bulbous cells of the mesotesta (Fig. 4E). The chalazal region has no evident mesotestal modification and no chalazal chamber or chalazal mucro exists. The exotesta is a single layer of palisade cells that are not uniform across the entire seed coat. The mesotesta contains large bulbous cells, and the endotesta is a uniform layer of square cells, but whether they are sclereids or parenchyma is unknown (Fig. 6R). An endotestal gap (side?) and CPG cells are present, but difficult to see in the material examined. The embryo is straight and does not come into contact with the endotesta.

Burbidgea *Hook.f. (one species analysed)*
Burbidgea stenantha Ridl. seeds are ellipsoid, taper at the base and have a striated surface. They are more than twice as long as they are wide and have no noticeable external raphe groove or chalazal indentation. The micropylar collar is formed from a single layer of cells and the operculum comprises two distinct layers, the outer of which corresponds to the layer of bulbous cells in the mesotesta. A hilar rim and a micropylar proliferation of mesotesta cells are present. The chalazal region is modified into a chalazal mucro (Fig. 5H) and an endotestal gap with CGP cells is present on the side of the seed. The seed coat comprises a uniform palisade exotesta, mesotesta of bulbous cells and a uniform endotesta of square sclereids. The embryo is straight and does not come into contact with the endotesta.

Pleuranthodium *(K.Schum.) R.M.Sm. (unknown species analysed)*
Pleuranthodium seeds are variously shaped, but the samples investigated are irregularly oblate with a wide equatorial region, and are striated and shiny (Fig. 2M, N). They are less than twice as long as they are wide and contain a chalazal indentation, but lack an external raphe groove. The micropylar collar comprises two distinct layers and the operculum is also two-layered, with an outer layer of bulbous mesotestal cells. A hilar rim, micropylar proliferation and chalazal mucro are all absent. The chalazal region contains a mesotestal proliferation of cells, but lacks a chalazal chamber. The exotesta is uniform and palisade, and a bulbous layer of mesotesta is present. The endotesta is also uniform and formed from square sclereids (Fig. 6J). An endotestal gap and CPG cells are present at the base of the seed. The embryo is straight and does not touch the inner layer of the endotesta.

Siamanthus *K.Larsen & J.Mood (one species analysed)*
Siamanthus siliquosus K.Larsen & J.Mood seeds are ovoid, taper at the base and have a verrucose surface. They are not more than twice as long as they are wide and lack an external raphe groove and chalazal indentation. The micropylar collar is formed from the endotesta only and the operculum comprises two layers. A hilar rim, micropylar and chalazal proliferation of cells, and a chalazal mucro, are lacking. The exotesta is made up of palisade cells, but is not uniform throughout the seed coat. The mesotesta consists of bulbous cells and the endotesta is a uniform layer of rectangular sclerenchymatous cells. An endotestal gap and CPG cells are present at the base of the seed. The embryo is L-shaped, but does not come into contact with the endotesta.

Siliquamomum *clade (clade 'b', one genus/one species analysed)*
Seeds of *Siliquamomum tonkinense* Baill. are ellipsoid, taper at the base and have a striate seed surface (Fig. 2Q, R). They are more than twice as long as they are wide and have a distinct external raphe, but no chalazal indentation. A micropylar collar formed from endotestal and mesotestal cells is present, as is a hilar rim. A micropylar mesotestal proliferation of cells is absent and the operculum is formed from a single layer of cells. No apparent chalazal mesotesta modification exists in this taxon, but a distinct chalazal mucro is present at the base of the seed (Fig. 5I). The exotesta is uniform and palisade, and a mesotesta of bulbous cells is lacking. The endotesta is also uniform and comprises a single layer of rectangular sclereids. An endotestal gap is present on the side of the seed and is oval shaped. The embryo is straight, elongated past the endotestal gap and does not come into contact with the endotesta.

Alpinia galanga *clade (clade 'c', one genus/three species analysed)*
Seeds of the *Alpinia galanga* clade are oblate, do not taper and have a shiny striated surface in *A. galanga* (L.) Willd., shiny(?) surface in *A. conchigera* Griff. and verrucose surface in *A. nigra* (Gaertn.) Burtt. They are less than twice as long as they are wide and contain no external raphe groove (present in *A. nigra*) or chalazal indentation. The micropylar collar is formed from mesotesta and endotesta. A hilar rim has not been observed. The operculum is two-layered in *A. conchigera* and *A. nigra*, but is made up of a single layer in *A. galanga*. The mesotesta is not proliferated in the micropylar region, but is differentiated into a small group of cells in the chalazal region in all three species studied. A chalazal chamber and chalazal mucro are lacking. The endotesta is uniform and

palisade in *A. conchigera* and *A. galanga*, but is not uniform or palisade in *A. nigra*. The mesotesta comprises large-bodied cells and the endotesta is uniform in all taxa. The endotesta in *A. nigra* is made up of square sclerenchymatous cells (Fig. 6M), whereas, in *A. conchigera* and *A. galangal*, they are rectangular in shape (Fig. 6F). Endotestal gaps and CPG cells occur at the base of the seed in all three taxa examined. The embryos of *A. conchigera* and *A. nigra* are basally bulbous (Fig. 7E), but L-shaped in *A. galanga*, and none touches the endotesta.

Amomum maximum *clade (clade 'd', one genus/two species analysed)*
Seeds of *Amomum* aff. *glabrum* S.Q.Tong are ellipsoid and rugose, and those of *A. sericeum* Roxb. are ovoid and striate. Tapering of the seed body is not evident in *A.* aff. *glabrum*, but is present at the base and apex of *A. sericeum*. In neither species examined is the seed more than twice as long as wide. An external raphe is present in *A. sericeum*, but lacking in *A.* aff. *Glabrum*, and neither shows evidence of an external chalazal indentation. A micropylar collar is present and formed from endotestal cells only (Fig. 4H). A distinct hilar rim and micropylar mesotestal proliferation are lacking. The operculum in both taxa is single-layered (Fig. 4H). A chalazal modification is absent in *A.* aff *glabrum*, but is present as a mesotestal proliferation of cells and an *Amomum*-type chalazal chamber in *A. sericeum* (Fig. 5D). A chalazal mucro is lacking in both species. The exotesta is uniform and palisade and the mesotesta is bulbous in *A. sericeum*, but absent in *A.* aff. *glabrum*. The endotesta is uniform and comprises rectangular-shaped sclereids. An endotestal gap and CPG cells are present at the base of the seed in *A.* aff. *glabrum*, but are located on the side of the seed in *A. sericeum*. The embryo of *A. sericeum* is L-shaped, whereas it is straight in *A.* aff. *glabrum*; neither embryo touches the endotesta.

Alpinia fax *clade (clade 'f', one genus/one species analysed)*
Alpinia fax has ellipsoid seeds that possess a shiny striate seed coat and do not taper. Seeds are less than twice as long as they are wide and lack an external raphe groove and chalazal indentation. The micropylar collar is formed from endotesta cells only and the operculum has two distinct cell layers. A hilar rim and mesotestal proliferation of cells are both absent (Fig. 3C, D). The chalazal region is characterized by a mesotestal proliferation of cells and an *Alpinia*-type chalazal chamber, but a chalazal mucro is not observed. The exotesta is a uniform layer of palisade cells, and the mesotesta is made up of large bulbous cells. The endotesta is also uniform and comprises rectangular sclereids. An endotestal gap and CPG cells are present on the side of the seed, and the embryo is straight and does not touch the seed coat.

Renealmia *L.f. clade (clade 'g', one genus/two species analysed)*
Renealmia seeds are striate and ellipsoid in *R. lucida* Maas, but ovoid in *R. occidentalis* (Sw.) Sweet. Both seeds taper at the base and are not more than twice as long as they are wide. An external raphe groove and a chalazal indentation are absent. The micropylar collar comprises endotesta and mesotesta and, in both taxa, a hilar rim is present, although it is much more pronounced in *R. lucida* (Fig. 4D). The operculum in both taxa is formed from two distinct layers of testa, and a micropylar mesotestal proliferation of cells is absent. In the chalazal region, a proliferation of mesotestal cells and an *Alpinia*-type chamber are evident in *R. lucida*, whereas *R. occidentalis* contains an *Amomum*-type chamber; both lack a chalazal mucro. The exotesta is uniform and palisade, and the mesotesta contains bulbous cells (Fig. 6K). The endotesta is uniform and comprises square sclereids with an endotestal gap and CPG cells at the base of the seed. The embryo of *R. lucida* is L-shaped, and is straight in *R. occidentalis*, but neither touches the inner wall of the endotesta.

Aframomum *K.Schum. clade (clade 'h', one genus/two species analysed)*
The *Aframomum* clade is characterized by ellipsoid seeds that taper towards the base and apex, and have a shiny, striate seed coat (Fig. 2B). Seeds are less than twice as long as they are wide and lack a raphe groove and chalazal indentation. The micropylar collar comprises both mesotesta and endotesta, and the operculum is made up of two distinct layers. A small hilar rim is evident, as are proliferations in the mesotestal cells in the micropylar region (Fig. 4A, B). The chalazal region is characterized by a symmetrical proliferation of mesotesta cells (Fig. 5A, B), and a chalazal chamber and chalazal mucro are absent. The exotesta comprises a uniform layer of palisade cells, a mesotesta of large-bodied cells and a uniform endotesta with square sclerenchymatous cells (Fig. 6A–C). An endotestal gap and CPG cells are present at the base of the seed. The embryo is straight and elongate, and does not touch the endotesta.

Geostachys *Ridl. clade (clade 'i', one genus/one species analysed)*
Geostachys densiflora Ridl. has an ovoid seed that tapers at the base and a verrucose seed surface. Seeds

are less than twice as long as they are wide and there is no external raphe groove or chalazal indentation. The micropylar collar is formed from a single layer of endotestal cells and the operculum has two distinct layers. A micropylar mesotestal proliferation and a hilar rim are both absent. The chalazal region has a proliferation of mesotestal cells and an *Amomum*-type chalazal chamber, but a chalazal mucro is lacking (Fig. 5F). The exotesta comprises palisade cells that are not uniform throughout the seed coat. The mesotesta is a layer of large bulbous cells and the endotesta is a uniform layer of rectangular sclereids. An endotestal gap and CPG cells are present and originate from tissues on the side of the seed. The embryo of *G. densiflora* is L-shaped and does not touch the endotesta.

Alpinia zerumbet *clade (clade 'k', four species analysed)*

Seeds of the *A. zerumbet* clade are oblate (*A. stachyodes* Hance), ellipsoid [*A. brevilabris* C.Presl and *A. japonica* (Thunb.) Miq.] or variously shaped [*A. aquatica* (Retz.) Roscoe], with a striate (in *A. aquatica* and *A. japonica*), shiny striate (*A. stachyodes*) or verrucose (*A. brevilabris*) surface, and lack obvious tapering (Fig. 2I, J, O, P). They are not more than twice as long as they are wide and may (*A. aquatica*, *A. brevilabris*, *A. stachyodes*; Fig. 2I, J, O, P) or possibly may not (*A. japonica*) have an external raphe groove. An external chalazal indentation is present in *A. aquatica*, *A. brevlabris* and *A. stachyodes*, but is unknown in *A. japonica*. Micropylar collars are either formed from endotesta and mesotesta (*A. aquatica*, *A. brevilabris* and *A. stachyodes*) or of endotestal cells only (*A. japonica*). Opercula in all species are two-layered. A micropylar mesotestal proliferation of cells and a hilar rim are both absent for all taxa analysed. The chalaza has no modifications in *A. aquatica* and *A. brevilabris*, a mesotestal proliferation lacking a chalazal chamber in *A. stachyodes* and a proliferation of cells and an *Alpinia*-type chalazal chamber in *A. japonica*. No seeds have chalazal mucros. The exotesta is uniform and palisade in *A. stachyodes*, uniform but not palisade in *A. aquatica*, and neither uniform nor palisade in *A. brevilabris* (Fig. 6N) and *A. japonica*. The mesotesta comprises large bulbous cells in all taxa sampled, and the endotesta is a uniform layer of square (*A. aquatica* and *A. brevilabris*) or rectangular (*A. japonica* and *A. stachyodes*) sclereids. CPG cells and an endotestal gap occur in all taxa and are either at the base (*A. stachyodes*) or at the side (*A. aquatica*, *A. brevilabris* and *A. japonica*). Embryos in all species examined are L-shaped and the embryo does not touch the endotesta in all taxa.

Alpinia zerumbet *subclade (clade 'ki', three species analysed)*

The seed shape ranges from ellipsoid [*A. haenkei* C.Presl and *A. malaccensis* (Burm.f.) Roscoe] to ovoid [*A. zerumbet* (Pers.) B.L.Burtt & R.M.Sm.], and is either striate (*A. haenki*) or verrucose (*A. malaccensis* and *A. zerumbet*). None of the species has a tapering seed body. In *A. malaccensis* only, the seeds are twice as long as they are wide. An external raphe is evident in all taxa sampled and extends down two sides of the seed (Fig. 2E, F), and is also found in *A. katsumadai* Hayata and *A. oblongifolia* Hayata, two taxa not included in recent molecular phylogenetic analyses (Kress *et al*., 2005, 2007). An external chalazal indentation, micropylar mesotestal proliferation of cells and hilar rim are lacking for all taxa sampled. A well-developed micropylar collar formed from endotesta and mesotesta, and an operculum comprising two distinct layers, are present in all species sampled. A chalazal mucro is not present, but a distinct chalazal modification of the mesotesta is present that forms a column of cells that splits the embryo chamber into two halves at the base (Fig. 5E). An *Alpinia*-type chalazal chamber is present at the top of the columnar mesotesta proliferation of cells in *A. haenkei* and *A. malaccensis*, whereas an *Amomum*-type chamber is present in *A. zerumbet*. The exotesta is palisade in *A. malaccensis* and *A. haenkei*, and is not a uniform layer in any taxon sampled. The mesotesta comprises large, bulbous cells and the endotesta is a uniform layer of square cells in *A. haenkei* and *A. zerumbet*, but rectangular in *A. malaccensis*. An endotestal gap is present at the base of each seed and is associated with CPG cells. All of the seeds have forked embryos that do not touch the endotesta (Fig. 7F, I).

Plagiostachys *Ridl. subclade (clade 'kii', one genus/two species analysed)*

Seeds in the *Plagiostachys* subclade are ovoid and striate (*P. escritorii* Elmer) or ellipsoid and striate (*P. philippinensis* Ridl.), with both forms tapering at the base. Neither species has seeds more than twice as long as they are wide and they do not have an external raphe grove or chalazal indentation. The micropylar collar is formed from endotesta only in *P. philippinensis* and of both endotesta and mesotesta in *P. escritorii*. The operculum comprises two distinct layers in both taxa, and a hilar rim and micropylar mesotestal proliferation of cells are absent. The chalazal region has both a mesotestal proliferation of cells and an *Amomum*-type chalazal chamber, but lacks a chalazal mucro in both species (Fig. 5C). The exotesta of *P. escritorii* is uniform and palisade, but is uniform and not palisade in *P. philippinensis*. Both have a mesotesta of bulbous cells, a uniform

endotesta of square sclereids, an endotestal gap, CPG cells located on the side of the seed and straight embryos that do not contact the endotesta.

Alpinia carolinensis *clade (clade 'l', one genus/two species analysed)*
Seeds in the *A. carolinensis* clade (*A. boia* Seem. and *A. carolinensis*) are ovoid and striate in *A. boia* (Fig. 2A), but shiny striate in *A. carolinensis*, and taper at the apex (*A. boia*) or base (*A. carolinensis*). Seeds are less than twice as long as they are wide and lack an external raphe groove and chalazal indentation. The micropylar collar comprises endotesta (*A. boia*) or endotesta and mesotesta (*A. carolinensis*). The operculum is formed from two distinct cell types (Fig. 3A, B). A hilar rim and micropylar mesotestal proliferation of cells are absent. The chalazal region lacks a chalazal mucro, but is modified with a proliferation of mesotesta and *Alpinia*-type chalazal chamber in *A. carolinensis*, and contains a proliferation of mesotesta and *Amomum*-type chalazal chamber in *A. boia*. The exotesta is palisade in both members of the clade, but is uniform in *A. carolinensis* and not uniform and wavy in *A. boia* (Fig. 6D). The mesotesta consists of bulbous cells and the endotesta is a uniform layer of rectangular sclerified cells. An endotestal gap is apparent on the side of the seed and CPG cells are present in both taxa, but difficult to distinguish in *A. carolinensis*. Embryos are elongate and L-shaped, and touch the endotesta in *A. boia* (Fig. 7G), but do not in *A. carolinensis*.

Alpinia eubractea *clade (clade 'n', two genera/three species analysed)*
Seeds are ellipsoid and verrucose [*Alpinia luteocarpa* Elmer and *A. caerulea* (R.Br.) Benth.] or range from ellipsoid to ovoid and shiny striate (*Vanoverberghia sepulchrei* Merr.). All specimens examined taper at the base and are less than twice as long as they are wide. An external raphe groove and chalazal indentation are only present in *A. caerulea*. The micropylar collar consists of endotesta and mesotesta, and opercula are formed from two distinct layers (Fig. 4G). A hilar rim, micropylar mesotestal proliferation and chalazal mucro are absent in all taxa surveyed. The chalazal region is not modified in *A. caerulea* and *A. luteocarpa*, but is modified into a mesotestal proliferation of cells in *V. sepulchrei*. The exotesta is uniform and palisade in *A. caerulea* and *V. sepulchrei* (Fig. 6L), and not uniform or palisade in *A. luteocarpa*. All taxa have a bulbous mesotesta and a uniform endotesta of square sclereids. An endotestal gap and CPG cells are present and on the side of the seed in all taxa analysed. The embryos range from straight (*V. sepulchrei*) to L-shaped (*A. caerulea* and *A. luteocarpa*), but in neither case do they touch the endotesta (Fig. 7H).

Hornstedtia *Retz. grade (clade 'o', one genus/two species analysed)*
Hornstedtia seeds are ellipsoid and may taper at the apex (*H. conica* Ridl.) or not [*H. leonurus* (J.Koenig) Retz.]. The seed surface is striate and seeds are not more than twice as long as they are wide. An external raphe and chalazal indentation are present. The micropylar collar is formed from endotestal cells only (*H. leonurus*) or from endotestal and mesotestal cells (*H. conica*). The operculum comprises two layers, and a hilar rim and micropylar mesotestal proliferation are both absent (Fig. 4I, J). A modified mesotesta in the chalazal region exists as a proliferation of cells in *H. conica,* but is lacking in *H. leonurus*. A chalazal mucro is absent in both species. The exotesta ranges from being a non-uniform layer of non-palisade cells in *H. leonurus* to a uniform layer of palisade cells in *H. conica*. The mesotesta is lacking in *H. leonurus*, but is a layer of bulbous cells in *H. conica*. The endotesta of both species is uniform and consists of elongate palisade sclereids (Fig. 6P, Q). An endotestal gap and CPG cells are also present and located at the base of the seed in both species examined. The embryos of both species are straight and do not contact the endotesta.

Etlingera *Giseke clade (clade 'p', one genus/three species analysed)*
Seeds range from being ovoid and tapering at the apex [*Etlingera linguiformis* (Roxb.) R.M.Sm. and *E. yunnanensis* (T.L.Wu & S.J.Chen) R.M.Sm.] to ellipsoid seeds that taper at both the base and apex [*E. elatior* (Jack) R.M.Sm.]. Seed surfaces are striate in *E. elatior* and verrucose in *E. linguiformis* and *E. yunnanensis.* No seed is more than twice as long as it is wide, and an external raphe and chalazal indentation are present in all specimens sampled (Fig. 2K, L). The micropylar collar is formed from endotestal cells only, and the operculum comprises a single layer in *E. elatior* and *E. yunnanensis* and two layers in *E. linguiformis* (Fig. 3E, F). A hilar rim and micropylar mesotestal proliferation are lacking in all species sampled, as is any evidence of a modification of chalazal cells, including a chalazal mucro (Fig. 5G). The exotesta is not a uniform layer of cells, and lacks palisade cells. The mesotesta is highly reduced and lacks large bulbous cells. The endotesta is uniform and in all species is notably elongate, forming a column of palisade cells that accounts for the majority of the thickness of the seed coat (Fig. 6O). An endotestal gap and CPG cells are present and located at the base of all taxa sampled (Fig. 5G). The embryo of *E. yunnanensis* is straight (Fig. 7A), but those of

E. elatior and *E. linguiformis* are L-shaped and none touch the inner layer of the endotesta.

Amomum villosum *clade (clade 'q', one genus/four species analysed)*
All seeds sampled in the *A. villosum* clade are ellipsoid. Seeds may taper at the apex (*A. koenigii* J.F.Gmel. and *A. ochreum* Ridl.) or not (*A. lappaceum* Ridl.). They are more than twice as long as wide in *A. lappaceum* and *A. ochreum*, but not so in *A. koenigii*. Seed coats are either striate (*A. ochreum* and *A. koenigii*) or verrucose (*A. lappaceum*). An external raphe groove and chalazal indentation are absent in all members. The micropylar collar is formed from endotesta cells only in *A. koenigii* and *A. lappaceum*, whereas, in *A. ochreum*, it includes both endotesta and mesotesta. The operculum consists of two distinct layers and a hilar rim was observed in *A. ochreum* only (Fig. 4F). A micropylar mesotestal proliferation of cells is absent, but two types of chalazal modification have been found. In the chalaza, a mesotestal proliferation of cells is present without a chalazal chamber in *A. lappaceum* and *A. koenigii*, and, in *A. ochreum*, a mesotestal proliferation of cells as well as an *Alpinia*-type chalazal chamber have been observed. A chalazal mucro is not present in any taxa sampled from this clade. The exotesta is palisade in all but *A. koenigii*, and is either uniform (*A. koenigii* and *A. lappaceum*) or not (*A. ochreum*, Fig. 6H). A large bulbous mesotesta is characteristic of this clade and is shared by all members. The endotesta is uniform and with sclereids that can be square (*A. ochreum*) or rectangular (*A. koenigii* and *A. lappaceum*). An endotestal gap with CPG cells is present and on the side in all taxa sampled. The embryo is straight and does not touch the inner layer of the endotesta.

Elettaria *Maton (one genus/one species analysed)*
Seeds of *Elettaria cardamomum* (L.) Maton are ellipsoid with no evident tapering. They have a rugose surface (Fig. 2D). They are less than twice as long as they are wide and possess a distinct external raphe groove, but no chalazal indentation (Fig. 2G, H). A hilar rim and micropylar mesotestal proliferation are absent, and the micropylar collar comprises endotestal cells only. The operculum consists of two distinct layers, and the chalazal region has a mesotestal proliferation of cells. The exotesta forms a uniform layer of palisade cells and, beneath it, is a layer of bulbous mesotesta. The endotesta is also uniform and comprises a single layer of rectangular sclereids. An endotestal gap and CPG cells on the side of the seed are both present in the chalazal region. The embryo is L-shaped and does not contact the inner endotestal wall.

DISCUSSION

Systematic significance of seeds of Alpinioideae

Seeds of Alpinioideae are quite variable in terms of their morphology and seed coat anatomy. When viewed in the context of a published phylogenetic analysis (Kress *et al*., 2007), we identified several characters of phylogenetic significance using three-dimensional visualizations and digital sections, many of which have not been documented previously in studies based on histological sections and surface fractures (e.g. Rodriguez-de la Rosa & Cevallos-Ferriz, 1994; Liao & Wu, 1996, 2000). Characters that most closely correspond with well-supported clades are the operculum layers, seed coat (testa) anatomy, location of the endotestal gap and structural variation in the chalazal and micropylar regions (Fig. 8). Characters that vary considerably in a clade and are therefore considered to be homoplasious are the seed length and surface.

The tribes Riedelieae and Alpinieae are quite similar in seed morphology and anatomy, and no characters were found to be exclusive to either tribe; however, the number of layers in the operculum was found to differentiate the two tribes, with the exception of three taxa. In both tribes, the operculum often comprises two layers (one-layered opercula being observed only in the *Amomum maximum* clade, *Etlingera elatior* and *Siliquamomum tonkinense*), with the inner layer derived from the endotesta and the outer layer from the mesotesta. In Alpinieae, the outer layer of the operculum is a torus or doughnut-shaped mass of cells that are indistinct in SRXTM images (Fig. 4A), but, in Riedelieae, the second layer consists of bulbous mesotestal cells that look very similar to the mesotesta in the seed coat (e.g. Fig. 4E, arrow), especially those cells that comprise the micropylar and chalazal mesotestal proliferations seen in some seeds. A few exceptions were found in the opercula structure, e.g. the operculum of *Siamanthus siliquosus* resembles Alpinieae in cell structure, and the opercula of *Alpinia luteocarpa* and *A. nigra* have bulbous cells more similar to Riedelieae.

The most distinct clades based on seed characters are the *Aframomum* clade, *Alpinia carolinensis* clade, *Alpinia galanga* clade, *Alpinia zerumbet* subclade, *Plagiostachys* subclade, *Amomum maximum* clade, *Etlingera* and *Renealmia* (Fig. 8). In contrast, the *Alpinia eubractea* clade, *Alpinia zerumbet* clade, *Amomum villosum* clade and *Hornstedtia* grade have considerable variation in seed morphology and anatomy, and share no combination of characters that are unique to these groups. The most informative characters were found in micropylar and chalazal mesotestal modifications, the location of the

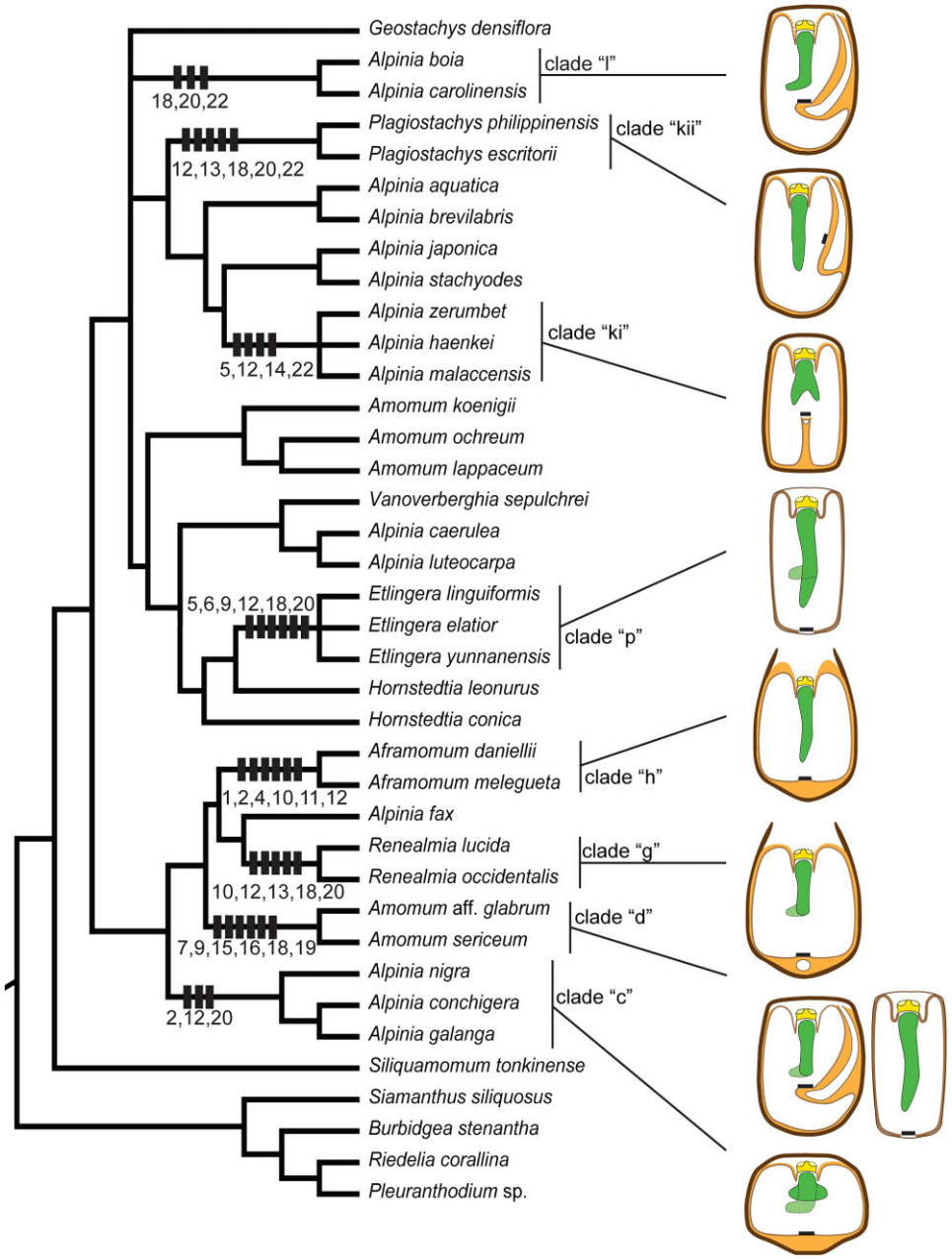

Figure 8. Phylogenetic tree for Alpinioideae based on Kress *et al*. (2007) with sampled taxa as terminals. Numbers along the branches indicate the characters that are distinctive; see text for details of state changes. Seed diagrams represent clades with distinct combinations of characters; embryo (green); operculum (endotestal layer, dark yellow; mesotestal layer, pale yellow); endotesta (light brown); mesotesta (tan); exotesta (dark brown); chalazal pigment group (black). Dotted lines indicate characters that were variable within a clade.

endotestal gap, and the shape of exotestal and endotestal cells. No characters were found to be exclusive of a single clade, but multiple clades in Alpinioideae share features or combinations of features only found within a single clade.

The *Aframomum* clade is identified as a strongly monophyletic lineage within Alpinioideae, and has a distinct flask-shaped fruit, a notable synapomorphy for the genus (Harris *et al*., 2000; Kress *et al*., 2005). Seeds of the genus are distinctive in having ellipsoid, shiny, striated seeds that are less than twice as long as wide. The presence of a hilar rim and micropylar mesotesta proliferation is exclusive to *Aframomum* spp. (*Aframomum* clade) and *Burbidgea stenantha*

(Riedelieae), but these two genera are easily distinguished from one another by the presence of a second operculum layer of bulbous cells and the absence of a chalazal mucro in Alpinieae (absent and present, respectively, in *Burbidgea*).

The *Alpinia carolinensis* clade includes members with a caducous primary inflorescence bract, tightly clasping tubular bracteoles and a narrow fleshy labellum adpressed to the stamen (Kress *et al*., 2005, 2007). It is the only clade to have seeds with a uniform endotesta of rectangular sclereids, an endotestal gap on the sidewall of the seed and an L-shaped embryo. It shares these features with *Alpinia fax* and *Amomum sericum*, but *Alpinia fax* differs from *Alpinia boia* in having an *Alpinia*-type chalazal chamber, and differs from both *Alpinia boia* and *Alpinia carolinensis* in having a straight embryo. *Amomum sericeum* differs in having a micropylar collar and operculum derived from the endotesta only.

The *Alpinia eubractea* clade is a strongly supported monophyletic clade, but lacks morphological apomorphies (Kress *et al*., 2007). Seeds show considerable variation within the three taxa sampled and have no combination of characters that were found only in this group. Seeds vary in micropylar and chalazal mesotestal proliferations, endotesta sclereid shape and endotestal gap location, four characters that were found to be consistent in and informative for the identification of other clades.

The *Alpinia galanga* clade was also found to be strongly supported on the basis of molecular data, and contains members with distinct branched inflorescences, open bracteoles, a clawed labellum and thin-walled fruits with a hypodermis and large parenchymatous cells in the mesocarp (Liao & Wu, 1996; Kress *et al*., 2007). Seeds in this clade are uniform in shape (oblate), lack an external raphe groove (except *A. nigra*) and chalazal indentation, and are characterized by the presence of a mesotestal proliferation of cells in the chalazal region and the absence of a chalazal chamber. They also have endotestal gaps at the base of the seed and embryos that do not touch the endotesta. Similar features were found in *Alpinia aquatica* and *A. stachyodes*, but these taxa possess an external raphe groove and a distinct chalazal dimple, which are lacking in members of the *A. galanga* clade, with the exception of a raphe groove in *A. nigra*.

Members of the *Alpinia zerumbet* clade do not unanimously share any characters or combination of characters that are unique to the clade, but two subclades (*Alpinia zerumbet* subclade and *Plagiostachys* subclade) are both well supported on the basis of seed characters. The *Alpinia zerumbet* subclade is supported by several characters: the presence of a 'double' raphe groove (Fig. 2E, F) that extends down both sides of the seed, a columnar mesotestal proliferation of cells in the chalazal region (Fig. 5E) and a forked embryo that does not touch the endotesta. This particular combination of morphology was not seen in any other group and was found in all three taxa sampled. It was also found in *A. katsumadai* and *A. oblongifolia*, taxa not included in the molecular analysis of Kress *et al*. (2007). *Alpinia katsumadai* was assigned to section *Alpinia* subsection *Catimbium* (Horan.) R.M.Sm. by Smith (1990a) on the basis of morphological data, the same section as the species from the *Alpinia zerumbet* subclade studied here.

The *Plagiostachys* subclade also contains a combination of characters not seen in any other taxon. Seeds sampled have a chalazal mesotestal proliferation of cells, an *Amomum*-type chalazal chamber, square endotestal sclereids, an endotestal gap on the sidewall of the seed and straight embryos. *Alpinia boia*, *Amomum sericeum* and *Geostachys densiflora* have similar mesotestal proliferations and *Amomum*-type chalazal chambers, but they all differ from *Plagiostachys* spp. in having rectangular endotestal sclereids and L-shaped embryos. *Elettaria cardamomum* is also similar to *Plagiostachys* spp., but differs in endotestal shape (rectangular) and the endotestal gap location (at base).

The *Amomum maximum* clade is either sister to the *Elettariopsis* clade, or *Elettariopsis* is nested within the *Amomum maximum* clade based on molecular evidence (Xia *et al*., 2004; Kress *et al*., 2007; Droop, 2012). Seeds sampled from the *Amomum maximum* clade *sensu* Kress *et al*. (2007) have a micropylar collar formed from endotestal cells only, an operculum that comprises a single layer of cells, a uniform layer of palisade exotesta and a uniform layer of rectangular endotestal sclereids. Similar seeds are seen in *Etlingera elatior* and *E. yunnanensis*, but members of this genus differ in their palisade endotestal cells and lack a uniform palisade exotesta.

The *Amomum villosum* clade is characterized by echinate or smooth fruits, and has been recognized as a distinct clade in multiple analyses (Xia *et al*., 2004; Kress *et al*., 2007; Droop, 2012). However, members of this clade have a wide range of seed characters, and no character or combination of characters was found to characterize this clade.

Based on molecular data (Kress *et al*., 2007), *Etlingera* and *Hornstedtia* were recovered as a single clade with *Hornstedtia* forming a basal grade, and seeds surveyed within the two genera are similar. *Etlingera* seeds have an external chalazal groove, a chalazal indentation, a micropylar collar formed from endotestal cells, no apparent chalazal mesotesta proliferation, a palisade endotesta and an endotesta at the base of the seed. This combination of characters is only seen in *Etlingera* seeds; furthermore, the most distinct character, palisade endotestal sclereids, is

only found in *Etlingera* and *Hornstedtia*. Although *Etlingera* has characteristic seed morphoanatomy, the two *Hornstedtia* taxa sampled varied greatly, and seed structure was not found to be diagnostic in this grade.

Renealmia is a well-supported monophyletic genus in Alpinioideae (clade 'g' of Kress *et al.,* 2007). Seeds have a distinct hilar rim, a character shared with *Aframomum* spp. (clade 'h'), *Amomum ochreum* (clade 'q'), *Burbidgea stenantha* (Riedelieae) and *Siliquamomum tonkinense* (clade 'b'), but differ from these taxa by also having a chalazal mesotestal proliferation of cells, an *Alpinia*-type or *Amomum*-type chalazal chamber, an endotestal gap at the base of the seed and an endotesta of square sclereids. Stellate trichomes on vegetative structures and a basal inflorescence (terminal on leafy shoots in some species) are two characters that, in combination, have been identified previously as unique to *Renealmia* (Kress *et al*., 2007), and the combination of seed characters noted above adds additional support for this clade.

The identification of many taxa in Alpinieae, in particular those in *Alpinia*, is difficult, and few apomorphies exist in the newly revised clades of the tribe (Kress *et al*., 2005, 2007). Here, we show that a broad sample of seeds in the subfamily demonstrates considerable variation in seed structure within the group, and that distinctive combinations of seed characters occur in many of the clades recognized by Kress *et al*. (2007). This suggests that an expanded analysis of seed structure focusing on chalazal and micropylar seed structure, seed coat characters and operculum structure will be fruitful in gaining insights into seed evolution in the group.

Comparison with other Zingiberales

The most comprehensive study on seed coat anatomy in Zingiberales was by Rodriguez-de la Rosa & Cevallos-Ferriz (1994), who examined 13 species in six of the eight extant families. The seed coat structure we document in Alpinioideae is different from that in Musaceae, Strelitziaceae and Cannaceae, which all have rather uniformly sclerenchymatous layers (Rodriguez-de la Rosa & Cevallos-Ferriz, 1994). Heliconiaceae seed coats have been interpreted as either highly reduced layers in mature seeds, in which the endocarp forms a protective coat of the seed (Takhtajan, 1985; Simão, Scatena & Bouman, 2006), or as endotesta (Rodriguez-de la Rosa & Cevallos-Ferriz, 1994; R. M. Smith & J. C. Benedict, pers. observ.). Further study is needed to clarify whether this layer is of integumentary or fruit-wall origin. The seed coat structure of Lowiaceae has not been described in the literature. Seed coats of Marantaceae and Costaceae are similar to those of Zingiberaceae in being thin and often formed from a large sclerified endotesta with relatively little mesotesta or exotesta (Rodriguez-de la Rosa & Cevallos-Ferriz, 1994; Benedict, 2012).

Previous papers have documented the presence/absence of chalazal chambers, opercula and a hilar rim in other families of Zingiberales. Opercula are absent in Cannaceae and are reduced to absent in Strelitziaceae, Heliconiaceae and some Zingiberaceae (Zingiberoideae) (Grootjen & Bouman, 1981; Manchester & Kress, 1993; Rodriguez-de la Rosa & Cevallos-Ferriz, 1994). A hilar rim has only been reported in Musaceae (Manchester & Kress, 1993), making it interesting that we found it here for the first time in some Alpinioideae. Developmental studies are needed to determine whether these are homologous structures.

Chalazal chambers have been recognized only within Musaceae and Costaceae (Grootjen & Bouman, 1981; Manchester & Kress, 1993; Rodriguez-de la Rosa & Cevallos-Ferriz, 1994), and here we demonstrate their presence in Zingiberaceae for the first time. This character is not unique to a few taxa in Zingiberaceae, but is present in Zingiberoideae (Zingiberoideae data not shown), the *Alpinia carolinensis* clade, *A. zerumbet* clade and subclades, *Hornstedtia* and some members of the *Amomum villosum* and *Amomum maximum* clades, although morphologies vary considerably. We further recognize two distinct types of chalazal chamber: a small circular *Alpinia*-type chamber at the base of the seed (Fig. 5E) and a large *Amomum*-type chamber that often connects to a raphe canal that extends from the base of the seed upwards through the mesotesta to the micropyle (Fig. 5C, D, F). The chalazal chambers of Alpinioideae differ in structure from those of Costaceae and Musaceae, although all are located in the mesotesta. The chamber in Costaceae is small and forms a square or rectangle in longitudinal section, whereas the chamber in Musaceae is large, sometimes one-third or more of the seed, and the septum that divides it from the embryo sac is derived from the endotesta and inner integument (McGahan, 1961; Manchester & Kress, 1993; Benedict, 2012). Further developmental studies are needed to determine whether the chalazal structures found in these three families are, in fact, homologous. In addition, a mesotestal proliferation of cells in the chalazal region has been documented in at least one taxon of each clade studied here, with the exception of *Etlingera*. To date, this type of chalazal modification has not been reported for other families of Zingiberales, although a broader survey of seed anatomy in the order is needed.

There are many fossil seed taxa that have been attributed to Zingiberales, including *Spirematospermum* Chandler from the Cretaceous–Pliocene of

Eurasia and North America, *Striatornata sanantoniensis* Rodriguez-de la Rosa & Cevallos-Ferriz and *Tricostatocarpon silvapinedae* Rodriguez-de la Rosa & Cevallos-Ferriz from the Campanian of Mexico, '*Musa*' *cardiosperma* Jain from the Maastrichtian/Palaeocene of India, and *Ensete oregonense* Manchester & Kress from the Eocene of Oregon (Chandler, 1925; Jain, 1963; Manchester & Kress, 1993; Rodriguez-de la Rosa & Cevallos-Ferriz, 1994; Fischer *et al*., 2009). A clear relationship with any particular family has been difficult to resolve for all of these taxa, except *Ensete oregonense*, which is undoubtedly a member of Musaceae (Manchester & Kress, 1993). Although *Spirematospermum* was originally described as a member of Zingiberaceae based on the spirally striated seeds with distinctive palisade exotesta (Koch & Friedrich, 1971; Friis, 1988), the presence of a chalazal chamber in the fossils was later used to ally *Spirematospermum* with Musaceae (Manchester & Kress, 1993; Rodriguez-de la Rosa & Cevallos-Ferriz, 1994; Fischer *et al*., 2009). Our documentation of a chalazal chamber in Zingiberaceae weakens the current interpretation of *Spirematospermum* as allied with Musaceae, and indicates that the original placement of *Spirematospermum* in or allied to Zingiberaceae based on similarities of seed coat anatomy should be reconsidered. In addition to seed coat anatomy, phytoliths present in *Spirematospermum* are primarily silica sand and occasional globular phytoliths (Koch & Friedrich, 1971; Chen & Smith, 2013), which are similar to phytoliths characterized from Zingiberaceae, but are quite different from phytoliths observed in Musaceae (e.g. Chen & Smith, 2013).

CONCLUSION

Seeds of Alpinioideae vary considerably in morphology and anatomy, and provide taxonomically useful characters for many recognized clades in the subfamily. Seeds of Riedelieae and Alpinieae are largely distinguishable based on the layering of the operculum. The most informative characters to distinguish clades are micropylar and chalazal mesotestal modifications, the location of the endotestal gap and the shape of endotestal and exotestal cells. Some clades were not distinguishable by seed characters alone (*Alpinia eubractea* clade, *Alpinia zerumbet* clade, *Amomum villosum* and the *Hornstedtia* grade), but many were easily recognized for their distinctive seeds (*Aframomum* clade, *Alpinia carolinensis* clade, *Alpinia galanga* clade, *Alpinia zerumbet* subclade, *Plagiostachys* subclade, *Amomum maximum* clade, *Etlingera* and *Renealmia*). This suggests that an expanded sampling of seeds, in particular those of clades not represented in the current study, will provide more details on the natural variation in the group and a deeper understanding of the evolution of Alpinioideae. In addition, seed data of extant members are critical to resolve the largely enigmatic fossil record of Zingiberales, which is rich in fruits and seeds.

ACKNOWLEDGEMENTS

The authors would like to thank A. Reznicek (MICH), W. J. Kress, I. Lopez and J. Wen (US), W. Friedrich (Aarhus University) and J. Kallunki and S. Sylva (NY) for facilitating access to material that formed part of this study, M. Andrew, G. Benson-Martin, S. Brown, J. Defontes, J. Dorey, S. Joomun, S. Little, A. Pineyro, S. McKechnie, K. Morioka, M. Ng, B. Robson, N. Sheldon and R. Yockteng for help at the beamlines, and G. Hodges and L. Tomlin for help with seed photography. Funding was provided from the Heliconia Society International award (J.C.B), Integrated Infrastructure Initiative (I3) on Synchrotrons and FELs through SLS to M.E.C. and S.Y.S., and National Science Foundation grants DEB 1257080 (S.Y.S.) and 1257701 (C.D.S.). The research of J.L.S. is supported by National Parks Board, Singapore and the Czech Science Foundation, GAČR P506-14-13541S. S.Y.S. completed part of this study during the tenure of a fellowship from the Michigan Society of Fellows, which is gratefully acknowledged. A portion of this work was included in the PhD dissertation of J.C.B. mentored by K. B. Pigg, whom J.C.B. would like to thank. This research used resources of the Advanced Photon Source, a US Department of Energy (DOE) Office of Science User Facility operated for the DOE Office of Science by Argonne National Laboratory under Contract No. DE-AC02-06CH11357. The Advanced Light Source is supported by the Director, Office of Science, Office of Basic Energy Sciences, of the US Department of Energy under Contract No. DE-AC02-05CH11231. The research leading to these results has received funding from the European Community's Seventh Framework Programme (FP7/2007-2013) under grant agreement n.°312284 (CALIPSO).

REFERENCES

Benedict JC. 2012. Zingiberalean fossils from the Late Paleocene of North Dakota, USA and their significance to the origin and diversification of Zingiberales. PhD Dissertation, Arizona State University.

Benedict JC, Pigg KB, DeVore ML. 2008. *Hamawilsonia boglei* gen. et sp. nov. (Hamamelidaceae) from the Late Paleocene Almont flora of central North Dakota. *International Journal of Plant Sciences* **169:** 687–700.

Berger F. 1958. Zur Samenanatomie der Zingiberazeen-Gattungen *Elettaria, Amomum* und *Aframomum*. *Scientia Pharmaceutica* **26:** 224–258.

Burtt BL. 1972. General introduction to papers on Zingiberaceae. *Notes from the Royal Botanical Garden Edinburgh* **31:** 155–166.

Chandler MEJ. 1925. *The Upper Eocene flora of Hordle, Hants*. London: Palaeontographical Society.

Chen ST, Smith SY. 2013. Phytolith variability in Zingiberales: a tool for the reconstruction of past tropical vegetation. *Palaeogeography, Palaeoclimatology, Palaeoecology* **370:** 1–12.

Chen SW, Lai MX, Qin DH, Fang D. 1989. Study on morphological tissues and essential oils of the adulterants of Sharen in *Amomum*. *China Journal of Chinese Materia Medica* **14:** 9–12.

Dowd BA, Campbell GH, Marr RB, Nagarkar V, Tipnis S, Axe L, Siddons DP. 1999. Developments in synchrotron x-ray computed microtomography at the National Synchrotron Light Source. *Proceedings of SPIE* **3772:** 224–236.

Droop AJ. 2012. Systematic and biogeographic studies in the genus *Amomum* Roxb. (Zingiberaceae) in Sumatra. DPhil Thesis, Aberdeen.

Fischer TC, Butzmann R, Meller B, Rattei T, Newman M, D Holscher C. 2009. The morphology, systematic position and inferred biology of *Spirematospermum* – an extinct genus of Zingiberales. *Review of Palaeobotany and Palynology* **157:** 391–426.

Friis EM. 1988. *Spirematospermum chandlerae* sp. nov., an extinct species of Zingiberaceae from the North American Cretaceous. *Tertiary Research* **9:** 7–12.

Grootjen CJ, Bouman F. 1981. Development of the ovule and seed in *Costus cuspidatus*, with special reference to the formation of the operculum. *Botanical Journal of the Linnean Society* **83:** 27–39.

Harris DJ, Newman MF, Hollingsworth ML, Moller M, Clark A. 2006. The phylogenetic position of *Aulotandra* (Zingiberaceae). *Nordic Journal of Botany* **23:** 725–734.

Harris DJ, Poulsen AD, Frimodt-Møller C, Preston J, Cronk QCB. 2000. Rapid radiation in *Aframomum* (Zingiberaceae): evidence from nuclear ribosomal DNA internal transcribed spacer (ITS) sequences. *Edinburgh Journal of Botany* **57:** 377–395.

Hass H, Rowe NP. 1999. Thin sections and wafering. In: Jones TP, Rowe NP, eds. *Fossil plants and spores: modern techniques*. London: Geological Society, 76–81.

Holttum RE. 1950. The Zingiberaceae of the Malay Peninsula. *Gardener's Bulletin of Singapore* **13:** 1–249.

Humphrey JE. 1896. The development of the seed in the Scitamineae. *Annals of Botany* **37:** 1–40.

Jain RK. 1963. Studies in Musaceae. I. *Musa cardiosperma* sp. nov., a fossil banana fruit from the Deccan Intertrappean Series, India. *Palaeobotanist* **12:** 45–54.

Kaewrsi W, Paisooksantivatana Y, Veesommai U, Eiadthong W, Vajrodaya S. 2007. Phylogenetic analysis of Thai *Amomum* (Alpinioideae: Zingiberaceae) using AFLP markers. *Kasetsart Journal: Natural Sciences* **41:** 213–226.

Koch BE, Friedrich WL. 1971. Früchte und Samen von *Spirematospermum* aus der Miozänen Fasterholt-Flora in Dänemark. *Palaeontographica Abteilung B* **136:** 1–46.

Kress WJ. 1990. The phylogeny and classification of Zingiberales. *Annals of the Missouri Botanical Garden* **77:** 698–721.

Kress WJ, Liu A-Z, Newman M, Li Q-J. 2005. The molecular phylogeny of *Alpinia* (Zingiberaceae): a complex and polyphyletic genus of gingers. *American Journal of Botany* **92:** 167–178.

Kress WJ, Newman MF, Poulsen AD, Specht CD. 2007. An analysis of generic circumscriptions in tribe Alpinieae (Alpinioideae: Zingiberaceae). *Gardens' Bulletin Singapore* **59:** 113–128.

Kress WJ, Prince LM, Hahn WJ, Zimmer EA. 2001. Unraveling the evolutionary radiation of the families of Zingiberales using morphological and molecular evidence. *Systematic Biology* **50:** 926–944.

Kress WJ, Prince LM, Williams KJ. 2002. The phylogeny and a new classification of the gingers (Zingiberaceae): evidence from molecular data. *American Journal of Botany* **89:** 1682–1696.

Larsen K. 2005. Distribution patterns and diversity centres of Zingiberaceae in SE Asia. *Biologiske Skrifter* **55:** 219–228.

Larsen K, Lock JM, Maas H, Mass PJM. 1998. Zingiberaceae. In: Kubitzki K, ed. *The families and genera of vascular plants, Vol. 4*. Berlin: Springer Press, 474–495.

Larsen K, Mood J. 1998. *Siamanthus*, a new genus of Zingiberaceae from Thailand. *Nordic Journal of Botany* **18:** 393–397.

Liao JP, Tang Y, Ye XL, Wu QG. 2004. Seed anatomy and its systematic significance in banana families of Zingiberales. *Journal of Tropical and Subtropical Botany* **12:** 291–297.

Liao JP, Wu QG. 1994. Anatomy and histochemistry of the seeds of *Amomum maximum*. *Journal of Tropical and Subtropical Botany* **2:** 58–66.

Liao JP, Wu QG. 1996. The significance of the seed anatomy of Chinese *Alpinia*. In: Wu TL, Wu QG, Chen ZY, eds. *Proceedings of the 2nd symposium on the family Zingiberaceae*. Guangzhou: Zhongshan University Press, 92–106.

Liao JP, Wu QG. 2000. A preliminary study of the seed anatomy of Zingiberaceae. *Botanical Journal of the Linnean Society* **134:** 287–300.

MacDowell AA, Parkinson DY, Haboub A, Schaible E, Nasiatka JR, Yee CA, Jameson JR, Ajo-Franklin JB, Brodersen CR, McElrone AJ. 2012. X-ray microtomography at the advanced light source. *Proceedings of SPIE* **8506:** 850618-1–850618-14.

Manchester SR, Kress WJ. 1993. *Ensete oregonense* sp. nov. from the Eocene of western North America and its phylogeographic significance. *American Journal of Botany* **80:** 1264–1272.

Marone F, Münch B, Stampanoni M. 2010. Fast reconstruction algorithm dealing with tomography artifacts. *SPIE Proceedings 'Developments in X-Ray Tomography VII'* **7804:** 1–11. doi:10.1117/12.859703.

Marone F, Stampanoni M. 2012. Regridding reconstruction algorithm for real-time tomographic imaging. *Journal of Synchrotron Radiation* **19:** 1029–1037.

Mauritzon J. 1936. Samenbau und Embryologie einiger Scitamineen. *Lunds Universitets Arsskrift* **31:** 1–31.

McGahan MW. 1961. Studies on the seed of banana. I. Anatomy of the seed and embryo of *Musa balbisiana*. *American Journal of Botany* **48:** 230–238.

Netolitzky F. 1926. Anatomie der Angiospermen-Samen. In: Linsbauer K, ed. *Handbuch pflanzen anatomie, Vol. 10*. Berlin: Gebrüder Borntraeger, 1–364.

Pedersen LB. 2003. Phylogenetic analysis of the subfamily Alpinioideae (Zingiberaceae), particularly *Etlingera* Giseke, based on nuclear and plastid DNA. *Plant Systematics and Evolution* **245:** 239–258.

Rangsiruji A, Newman MF, Cronk QCB. 2000a. Origin and relationships of *Alpinia galanga* (Zingiberaceae) based on molecular data. *Edinburgh Journal of Botany* **57:** 9–37.

Rangsiruji A, Newman MF, Cronk QCB. 2000b. A study of the infrageneric classification of *Alpina* (Zingiberaceae) based on the ITS region of nuclear rDNA and the *trn*L-F spacer of chloroplast DNA. In: Wilson KL, Morrison DA, eds. *Monocots – systematics and evolution*. Collingwood, Vic.: CSIRO Publishing, 695–709.

Rasband WS. 1997–2014. ImageJ. US National Institutes of Health, Bethesda, MD, USA. Available at: http://imagej.nih.gov/ij/

Ridley HN. 1909. Fruit of *Burbidgea*. *Journal of the Straits Branch of the Royal Asiatic Society* **53:** 175–176.

Rodriguez-de la Rosa R, Cevallos-Ferriz SRS. 1994. Upper Cretaceous zingiberalean fruits with in situ seeds from southeastern Coahuila, Mexico. *International Journal of Plant Sciences* **155:** 786–805.

Schumann K. 1904. Zingiberaceae. *Das Pflanzenreich* **4:** 1–458.

Simão DG, Scatena VL, Bouman F. 2006. Developmental anatomy and morphology of the seed of *Heliconia* (Heliconiaceae, Zingiberales). *Plant Biology* **8:** 143–154.

Smith RM. 1972. The genus *Burbidgea*. *Notes from the Royal Botanic Garden Edinburgh* **31:** 297–306.

Smith RM. 1990a. *Alpinia* (Zingiberaceae): a proposed new infrageneric classification. *Edinburgh Journal of Botany* **47:** 1–75.

Smith RM. 1990b. *Psychanthus* (K. Schum.) Ridley (Zingiberaceae): its acceptance at generic level. *Edinburgh Journal of Botany* **47:** 77–82.

Stampanoni M, Groso A, Isenegger A, Mikuljan G, Chen Q, Bertrand A, Henein S, Betemps R, Frommherz U, Bôhler P, Meister D, Lange M, Abela R. 2006. Trends in synchrotron-based tomographic imaging: the SLS experience. *Proceedings of SPIE* **6318:** 63180M.

Takhtajan A. 1985. *Comparative anatomy of seeds, Vol. I*. Leningrad: Izdat Nauka.

Tang Y, Xie Z, Liao J, Wu QG. 2005. Anatomy and histochemistry of the seeds in ginger families of Zingiberales and their systematic significances. *Acta Botanica Boreali-Occidentalia Sinica* **25:** 343–354.

The Plant List. 2013. Version 1.1. Published on the Internet. Available at: http://www.theplantlist.org/ (accessed 1 January 2013).

Thiers B. [continuously updated]. Index Herbariorum: a global directory of public herbaria and associated staff. New York Botanical Garden's Virtual Herbarium. Available at: http://sweetgum.nybg.org/ih/

Tschirch A. 1891. Physiologische Studien uber die Samen, inbesondere die Saugorgane derselben. *Annales du Jardin botanique de Buitenzorg* **8:** 143–145.

Wu TL. 1981. Zingiberaceae. *Flora Reipublicae Popularis Sinicae* **16:** 26–153.

Xia YM, Kress WJ, Prince LM. 2004. A phylogenetic analysis of *Amomum* (Alpinioideae: Zingiberaceae) using ITS and *mat*K DNA sequence data. *Systematic Botany* **29:** 334–344.